

# Fast quantum measurement tomography with dimension-optimal error bounds

Leonardo Zambrano,<sup>1,\*</sup> Sergi Ramos-Calderer,<sup>2,3</sup> and Richard Kueng<sup>4</sup>

<sup>1</sup>*ICFO - Institut de Ciències Fotoniques, The Barcelona Institute of Science and Technology, 08860 Castelldefels, Barcelona, Spain*

<sup>2</sup>*Centre for Quantum Technologies, National University of Singapore, Singapore.*

<sup>3</sup>*Quantum Research Center, Technology Innovation Institute, Abu Dhabi, UAE*

<sup>4</sup>*Department of Quantum Information and Computation at Kepler (QUICK), Johannes Kepler University Linz, 4040 Linz, Austria*

(Dated: July 8, 2025)

We present a two-step protocol for quantum measurement tomography that is light on classical co-processing cost and still achieves optimal sample complexity in the system dimension. Given measurement data from a known probe state ensemble, we first apply least-squares estimation to produce an unconstrained approximation of the POVM, and then project this estimate onto the set of valid quantum measurements. For a POVM with  $L$  outcomes acting on a  $d$ -dimensional system, we show that the protocol requires  $\mathcal{O}(d^3 L \ln(d)/\epsilon^2)$  samples to achieve error  $\epsilon$  in worst-case distance, and  $\mathcal{O}(d^2 L^2 \ln(dL)/\epsilon^2)$  samples in average-case distance. We further establish two almost matching sample complexity lower bounds of  $\Omega(d^3/\epsilon^2)$  and  $\Omega(d^2 L/\epsilon^2)$  for any non-adaptive, single-copy POVM tomography protocol. Hence, our projected least squares POVM tomography is sample-optimal in dimension  $d$  up to logarithmic factors. Our method admits an analytic form when using global or local 2-designs as probe ensembles and enables rigorous non-asymptotic error guarantees. Finally, we also complement our findings with empirical performance studies carried out on a noisy superconducting quantum computer with flux-tunable transmon qubits.

## I. INTRODUCTION

Quantum measurement tomography (QMT), also known as quantum detector tomography, is a key tool in the characterization of quantum devices. It enables the reconstruction of an unknown measurement process, typically modeled as a positive operator-valued measure (POVM), from experimental statistics. As quantum technologies advance, efficient and accurate measurement characterization becomes increasingly important to ensure the reliability of quantum experiments.

Several approaches to QMT have been proposed and implemented over the years [1–9]. These methods collect statistics from a set of known probe states and then infer a POVM via classical co-processing. A common strategy is to fit the POVM by solving a constrained optimization problem that minimizes the discrepancy between the observed frequencies and those predicted by the estimated POVM [1–7]. While such techniques, including maximum likelihood estimation and fitting using convex optimization, are widely used and often accurate, they become computationally expensive as the system dimension grows. Additionally, existing convergence guarantees for the estimated POVM are only valid in the asymptotic regime, where the central limit theorem applies. Note that this means that for finite sample sizes, error bars are not necessarily grounded in valid theory. Least-squares estimation (LSE) combined with projective methods offers a less computationally demanding alternative [8–11] and allows simpler derivation of reconstruction

error bounds. What is more, these error bounds also apply to the non-asymptotic setting.

Determining the sample complexity of QMT, that is, the number of POVM uses required to reconstruct a measurement with a given accuracy, is a fundamental challenge. Similar to quantum state tomography [12–19], such analysis enables the development of protocols that minimize the use of physical resources. This is particularly important in scenarios where time, memory, or access to quantum devices is limited. Therefore, studying sample complexity supports the design of optimized protocols, supporting practical applications in quantum computing and the experimental verification of quantum devices.

Given the rapid advance in the size of controllable quantum architectures, it is desirable to develop methods that are optimal in terms of sample complexity and also efficient in classical co-processing cost (think: memory and runtime). In this paper, we propose a two-step protocol that separates the estimation and constraint satisfaction processes within QMT to obtain an overall more computationally efficient reconstruction protocol. Following data acquisition, we use LSE to obtain an initial estimate of a POVM. LSE provides a computationally simple method to extract matrices that approximate the POVM, but without enforcing the required physical constraints. In a second step, we project this estimate onto the set of valid POVMs, ensuring that the final reconstructed operator satisfies all necessary conditions.

Our main contribution lies in analyzing the sample complexity of the aforementioned two-step protocol and proving that its scaling with the Hilbert space dimension matches fundamental lower bounds from quantum information theory. More precisely, for a POVM on a  $d$ -

\* [leonardo.zambrano@icfo.eu](mailto:leonardo.zambrano@icfo.eu)

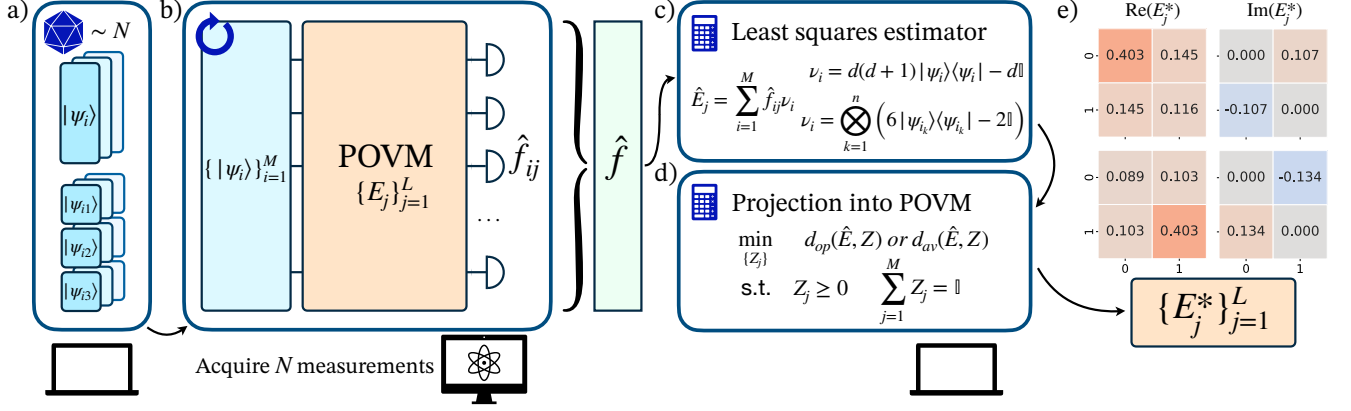


FIG. 1. Sketch of the quantum measurement tomography protocol. a) Uniformly sample a set of input states from an IC ensemble  $\{|\psi_i\rangle\}$  b) A quantum device is initialized in each randomized input state and measured using the POVM. The resulting frequencies  $\hat{f}_{ij}$  for input state  $|\psi_i\rangle$  and POVM outcome  $E_j$  are stored in a vector  $\hat{f}$ . c) A least-squares estimator for the POVM is computed using the measured frequencies  $\hat{f}$  and the operators  $\nu_i$ . This step depends on the choice of ensemble, such as a global or local 2-design. d) The raw least squares estimate is projected into the physical subspace of all POVMs via convex optimization. This produces the reconstructed POVM  $(E_1^*, \dots, E_L^*)$  as output. e) Example of the two first elements of a single qubit Symmetrical Informationally Complete (SIC-)POVM reconstructed from an experimental implementation on two flux-tunable transmon qubits.

dimensional system with  $L$  outcomes, we show that our protocol requires  $\mathcal{O}(d^3 L \ln(d)/\epsilon^2)$  samples to achieve error  $\epsilon$  in a worst-case distance, and  $\mathcal{O}(d^2 L^2 \ln(dL)/\epsilon^2)$  in an average-case distance. Conversely, we prove that *any* protocol based on independent, non-adaptive measurements must use the POVM at least  $\Omega(d^3/\epsilon^2)$  times to achieve the same error in worst-case distance, and  $\Omega(d^2 L/\epsilon^2)$  in average-case distance. Thus, our protocol achieves optimal sample complexity in the dimension  $d$  up to logarithmic factors.

To evaluate the reconstruction error, we consider two natural distance measures between POVMs. The *operational distance* quantifies the worst-case distinguishability of measurement outcomes and is commonly used in discrimination and error-mitigation tasks [20–23]. In contrast, the *average-case distance* captures the expected total variation distance between output distributions when input states are drawn from a random ensemble [23]. This measure reflects the typical performance of the POVM in practical scenarios.

Empirical performance evaluations are performed on a noisy quantum system, where experimentally implemented POVMs on two flux-tunable transmon qubits are successfully recovered using the presented protocol. By establishing the sample-optimality of our protocol and validating its performance in real settings, we offer both rigorous theoretical guarantees and a practical tool for quantum measurement characterization.

## II. PRELIMINARIES

In quantum mechanics, measurements are commonly described using the framework of positive operator-

valued measures, or POVMs for short. For a quantum system of dimension  $d$ , a POVM  $E$  is a collection of linear operators  $\{E_j\}_{j=1}^L$  acting on  $\mathbb{C}^d$  that satisfy the conditions

$$\sum_{j=1}^L E_j = \mathbb{I} \quad \text{and} \quad E_j \geq 0 \quad (1)$$

for every  $j = 1, 2, \dots, L$ . Here,  $E_j \geq 0$  requires that each operator is positive semidefinite, i.e.  $E_j^* = E_j$  (Hermitian) and every eigenvalue is nonnegative. When a quantum state  $\rho$  is measured using  $E$ , the probability of outcome  $j$  is given by the Born rule  $p_j = \text{tr}(\rho E_j)$ . The conditions in Eq. (1) ensure that this is a valid probability distribution, regardless of the quantum state  $\rho$ . Note that these probabilities depend on both the state and the POVM in question. Hence, they can be used to perform quantum measurement tomography. In this task, the goal is to reconstruct an unknown POVM using the measurement statistics obtained by applying it to a set of known quantum states  $\{\rho_i\}_{i=1}^N$ .

To assess the accuracy of tomography, we need a way to quantify the difference between POVMs. One natural choice is the operational distance  $d_{op}$ , defined as the largest total variation distance between the probability distributions that two POVMs can produce when applied to the same quantum state [20–23].

**Definition 1** (Operational distance). Let  $E$  and  $F$  be two  $L$ -outcome POVMs acting on a Hilbert space of dimension  $d$ . We define the operational distance  $d_{op}$  as

$$d_{op}(E, F) = \max_{\rho \in \mathcal{D}(\mathcal{H})} \frac{1}{2} \sum_{j=1}^L |\text{tr}(E_j \rho) - \text{tr}(F_j \rho)|. \quad (2)$$

This is equivalent to

$$d_{\text{op}}(E, F) = \max_{x \in \mathcal{P}(L)} \left\| \sum_{k \in x} (E_k - F_k) \right\|, \quad (3)$$

where  $\mathcal{P}(L)$  is the power set of  $\{1, 2, \dots, L\}$  and  $\|A\|$  is the spectral norm of  $A$ , i.e. the largest matrix eigenvalue in modulus. The number  $d_{\text{op}}(E, F) \in [0, 1]$  is related to the optimal probability of distinguishing between measurements  $E$  and  $F$  without using entanglement with a larger auxiliary system.

Note that the operational distance is a worst case distance measure. Sometimes it is more relevant to compare the average-case behavior of quantum measurements. To capture this, we follow Ref. [23] and average the total variation distance of output distributions over states sampled from a suitable ensemble. If these states form a state 4-design, this average TV distance is closely related to the following compact expression, see [23, Theorem 2]

**Definition 2** (Average case distance). Let  $E$  and  $F$  be two  $L$ -outcome POVMs acting on a Hilbert space of dimension  $d$ . We define the squared average-case distance  $d_{\text{av}}^2$  as

$$d_{\text{av}}^2(E, F) = \frac{1}{2d} \sum_{i=1}^L \left( \|E_i - F_i\|_F^2 + (\text{tr}[E_i - F_i])^2 \right), \quad (4)$$

where  $\|A\|_F = \sqrt{\text{tr}[A^\dagger A]}$  denotes the Frobenious norm.

We base our constructive upper bounds on sufficient sample complexity on matrix-valued concentration inequalities. The matrix Bernstein inequality is arguably the most well-known example of this kind [24–26]. The following version is taken from Ref. [27].

**Theorem 1.** Let  $X_1, X_2, \dots, X_N$  be independent, zero mean  $d \times d$  Hermitian matrices such that  $\|X_j\| \leq K$  almost surely for all  $j$ . Then, for every  $\epsilon \geq 0$ , we have

$$\Pr \left( \left\| \sum_{j=1}^N X_j \right\| \geq \epsilon \right) \leq 2d \exp \left( -\frac{\epsilon^2/2}{\sigma^2 + K\epsilon/3} \right), \quad (5)$$

where  $\sigma^2 = \left\| \sum_{j=1}^N \mathbb{E} X_j^2 \right\|$ .

Finally, we base our unconditional lower bounds on the sample complexity required for any quantum measurement protocol on Fano's inequality. More precisely, we use the following consequence which is displayed in [18, Corollary 2.7].

**Lemma 2.** Let  $X$ ,  $Y$ , and  $\hat{X}$  be discrete random variables forming a Markov chain  $X \rightarrow Y \rightarrow \hat{X}$ , where  $X$  takes values in  $\mathcal{X}$ . Suppose Alice sends a message  $X \sim \text{Unif}(\mathcal{X})$  and Bob is able to decode the message with constant probability of success using  $\hat{X}$ . Then, it must hold that

$$I(X : Y) = \Omega(\log |\mathcal{X}|), \quad (6)$$

where  $I$  denotes the mutual information

### III. PROJECTED LEAST-SQUARES QUANTUM MEASUREMENT TOMOGRAPHY

Here, we present a protocol to reconstruct any  $L$ -outcome POVM on a  $d$ -dimensional system with a sample complexity of  $N \in \mathcal{O} \left( \frac{d^3 L}{\epsilon^2} \ln(d) \right)$  in the operational distance  $d_{\text{op}}$  (worst case), and  $N \in \mathcal{O} \left( \frac{d^2 L^2}{\epsilon^2} \ln(Ld) \right)$  in the average distance  $d_{\text{av}}$ . A sketch of this protocol, and a sample of reconstructed empirical data are shown in Fig. 1.

#### A. Protocol

Our aim is to characterize a POVM  $E$  with  $L$  elements  $\{E_1, E_2, \dots, E_L\}$  acting on a Hilbert space of dimension  $d$ . To this end, we collect measurement statistics from a known set of quantum states  $\{|\psi_i\rangle\}_{i=1}^M$ . This set is chosen to be informationally complete, meaning that for any POVM element  $E_j$ , the probabilities  $\langle \psi_i | E_j | \psi_i \rangle$  uniquely identify  $E_j$ . We then perform least-squares estimation to obtain preliminary estimators for the POVM elements, which are subsequently projected onto the set of physical POVMs.

It is worthwhile to point out that the least-squares estimation step can be computed analytically if the ensemble of states  $\{|\psi_i\rangle\}_{i=1}^M$  either form a global 2-design or are tensor products of single-qubit 2-designs. In the latter case, each state is of the form  $|\psi_i\rangle = |\psi_{i_1}\rangle \otimes |\psi_{i_2}\rangle \otimes \dots \otimes |\psi_{i_n}\rangle$ , where the states  $\{|\psi_{i_k}\rangle\}$  of each qubit  $k = 1, \dots, n$  form a 2-design. Examples of 2-designs include stabilizer states [28], states from a symmetric informationally complete POVM (SIC-POVM) [29], and states forming a maximal set of mutually unbiased bases (MUBs) [30]. We propose the following estimation protocol:

1. *Data collection.* We uniformly sample a state from the set  $\{|\psi_i\rangle\}_{i=1}^M$ , prepare it on the quantum device and then measure it using the POVM. This procedure is repeated  $N$  times, resulting in a list of relative frequencies  $\hat{f}$ , where  $\hat{f}_{ij}$  denotes the number of times the outcome associated with  $E_j$  is observed when preparing the state  $|\psi_i\rangle$ , divided by  $NM$ . These relative frequencies are unbiased estimators of the probabilities  $p_{ij} = \langle \psi_i | E_j | \psi_i \rangle / M$ .
2. *Least squares estimator.* We compute empirical estimators  $\hat{E}_j$  of each POVM element  $E_j$  separately and analytically as

$$\hat{E}_j = \sum_{i=1}^M \hat{f}_{ij} \nu_i, \quad (7)$$

where

$$\nu_i = d(d+1)|\psi_i\rangle\langle\psi_i| - d\mathbb{1} \quad (8)$$

if the set of states  $\{|\psi_i\rangle\}_{i=1}^M$  forms a 2-design (see App. A) or

$$\nu_i = \bigotimes_{k=1}^n (6|\psi_{i_k}\rangle\langle\psi_{i_k}| - 2\mathbb{1}) \quad (9)$$

if the set of states is a tensor product of single-qubit 2-designs (see App. B). The elements from Eq. (7) form an unbiased estimator for the POVM, denoted as  $\hat{E}$ .

3. *Projection onto a POVM.* The bare least squares estimator  $\hat{E} = \{\hat{E}_1, \dots, \hat{E}_L\}$  will typically not meet the conditions of a physical POVM. To obtain a physical object we solve the following convex optimization problem

$$\begin{aligned} & \underset{\{Z_1, \dots, Z_L\} \subset \mathbb{C}^{d \times d}}{\text{minimize}} && d_{\text{op}}(\hat{E}, Z) \text{ or } d_{\text{av}}(\hat{E}, Z) \\ & \text{subject to} && Z_j^\dagger = Z_j, \quad Z_j \geq 0 \\ & && \sum_{j=1}^M Z_j = \mathbb{1}. \end{aligned} \quad (10)$$

We output the optimal solution ( $\text{argmin}$ )  $\{E_j^*\}_{j=1}^L$  of this optimization problem as the estimator of the POVM in the correspondent distance.

### B. Error analysis for operational distance $d_{\text{op}}$

Now, we will show that the worst-case error  $d_{\text{op}}(E, E^*)$  can be controlled by the sample size  $N$ .

**Theorem 3.** *Assume an  $L$ -outcome POVM  $E$  acting on a Hilbert space dimension  $d$  and an IC set of states  $\{|\psi_i\rangle\}_{i=1}^M$ . To achieve a reconstruction error  $d_{\text{op}}(E, E^*) \leq \epsilon$  with probability  $1 - \delta$  using the protocol described above, the required sample size is*

$$N \geq \frac{8(d^3 + d^2(1 + \epsilon/6))}{\epsilon^2} \ln \left( \frac{2^{L+1}d}{\delta} \right) \quad (11)$$

if  $\{|\psi_i\rangle\}_{i=1}^M$  is a 2-design and

$$N \geq \frac{8(10^n + 4^n \epsilon/6)}{\epsilon^2} \ln \left( \frac{2^{L+1}2^n}{\delta} \right). \quad (12)$$

if the POVM acts on an  $n$ -qubit system and  $\{|\psi_i\rangle\}_{i=1}^M$  is a tensor product of single-qubit 2-designs.

These bounds imply that the sample complexity of our protocol scales as  $\mathcal{O}(d^3 L / \epsilon^2)$  when using global 2-designs, and as  $\mathcal{O}(d^{3.33} L / \epsilon^2)$  for tensor-product 2-designs (up to logarithmic factors). The number of degrees of freedom in an  $L$ -outcome POVM on a  $d$ -dimensional Hilbert space is  $\Omega(d^2 L)$ , so the required sample size is only a factor of  $d$  larger than this minimal parameter count.

*Proof.* The first step in the proof is to control the error in the least squares estimator  $\hat{E}$ , given by

$$d_{\text{op}}(E, \hat{E}) = \max_{x \in \mathcal{P}(L)} \left\| \sum_{j \in x} (\hat{E}_j - E_j) \right\|. \quad (13)$$

We will apply the matrix Bernstein inequality to each term in the maximization and then use the union bound to determine the number  $N$  of POVM uses required to ensure that  $d_{\text{op}}(E, \hat{E}) \leq \epsilon/2$  with confidence  $1 - \delta$ . Then, in a second step we will use this result to bound the error in the projected estimator  $E^*$  by  $\epsilon$ .

From Eqs. (7) and (13) we have

$$d_{\text{op}}(E, \hat{E}) = \max_{x \in \mathcal{P}(L)} \left\| \sum_{i=1}^M \hat{f}_i^{(x)} \nu_i - F^{(x)} \right\|, \quad (14)$$

where

$$F^{(x)} = \sum_{j \in x} E_j \quad \text{and} \quad \hat{f}_i^{(x)} = \sum_{j \in x} \hat{f}_{ij}. \quad (15)$$

Here,  $F^{(x)}$  is a POVM element that groups the outcomes  $j \in x$ , and  $\hat{f}_i^{(x)}$  represents the associated relative frequencies estimated using  $N$  shots.

Let  $\hat{X}^{(x)}$  be the random matrix that, for  $i = 1, \dots, M$ , takes the value  $\nu_i$  with probability  $p_i^{(x)} = \frac{1}{M} \langle \psi_i | F^{(x)} | \psi_i \rangle$  and takes the value zero with probability  $1 - \sum_i p_i^{(x)}$ . This allows us to rewrite the least-squares estimator in Eq. (14) as

$$\sum_{i=1}^M \hat{f}_i^{(x)} \nu_i = \frac{1}{N} \sum_{k=1}^N \hat{X}_k^{(x)}, \quad (16)$$

where each  $\hat{X}_k^{(x)}$  is an i.i.d. copy of  $\hat{X}^{(x)}$ .

For any subset  $x$  of  $\mathcal{P}(L)$ , we have that

$$\begin{aligned} \mathbb{E} \left( \hat{X}_k^{(x)} \right) &= \sum_{i=1}^M \frac{1}{M} \langle \psi_i | F^{(x)} | \psi_i \rangle \nu_i \\ &= F^{(x)}. \end{aligned} \quad (17)$$

Thus, we can apply the matrix Bernstein inequality, Eq. (5), to the matrices  $\frac{1}{N} (\hat{X}_k^{(x)} - F^{(x)})$ . To do this, we need the quantities  $K$  and  $\sigma^2$ . As shown in App. A, if the states  $\{|\psi_i\rangle\}_{i=1}^M$  form a 2-design, then  $K \leq d^2/N$  for all  $i$  and  $\sigma^2 \leq (d^3 + d^2)/N$ . Substituting these values in Eq. (5), we obtain

$$\begin{aligned} \Pr \left( \left\| \frac{1}{N} \sum_{k=1}^N \hat{X}_k^{(x)} - F^{(x)} \right\| \geq t \right) \\ \leq 2d \exp \left( - \frac{Nt^2/2}{d^3 + d^2(1 + t/3)} \right). \end{aligned} \quad (18)$$

We define  $\delta/2^L = 2d \exp\left(-\frac{Nt^2/2}{d^3+d^2(1+t/3)}\right)$ . Then, we find that for a given error  $t$  and confidence  $1-\delta$ , the number of shots required is

$$N \geq \frac{2(d^3 + d^2(1+t/3))}{t^2} \ln\left(\frac{2^{L+1}d}{\delta}\right). \quad (19)$$

Now we use the union bound over all  $2^L$  sets in  $\mathcal{P}(L)$ :

$$\begin{aligned} & \Pr\left(\exists x \in \mathcal{P}(L) : \left\|\frac{1}{N} \sum_{k=1}^N \hat{X}_k^{(x)} - F^{(x)}\right\| \geq t\right) \\ & \leq \sum_{x \in \mathcal{P}(L)} \Pr\left(\left\|\frac{1}{N} \sum_{k=1}^N \hat{X}_k^{(x)} - F^{(x)}\right\| \geq t\right) \\ & \leq 2^L \frac{\delta}{2^L} = \delta. \end{aligned} \quad (20)$$

Thus, if we want an error  $d_{\text{op}}(E, \hat{E})$  smaller than  $t = \epsilon/2$  with probability  $1-\delta$ , we need

$$N \geq \frac{8(d^3 + d^2(1+\epsilon/6))}{\epsilon^2} \ln\left(\frac{2^{L+1}d}{\delta}\right). \quad (21)$$

If the frame is composed of tensor products of single-qubit 2-designs, then, as shown in App. B,  $K \leq 4^n/N$  for all  $i$ , and  $\sigma^2 \leq 10^n/N$ . Following a similar calculation as above, if we require an error in  $d_{\text{op}}(E, \hat{E})$  smaller than  $\epsilon/2$  with probability  $1-\delta$ , we need

$$N \geq \frac{8(10^n + 4^n\epsilon/6)}{\epsilon^2} \ln\left(\frac{2^{L+1}2^n}{\delta}\right). \quad (22)$$

We have already established an error bound for the estimator  $\hat{E}$ . The next step is to derive a bound for the projected estimator  $E^*$ . Suppose the protocol is successful, meaning that  $d_{\text{op}}(E, \hat{E}) \leq \epsilon/2$ . In that case, the operational distance between the projected estimator  $E^*$  and the true POVM  $E$  satisfies

$$\begin{aligned} d_{\text{op}}(E, E^*) & \leq d_{\text{op}}(E, \hat{E}) + d_{\text{op}}(\hat{E}, E^*) \\ & \leq 2d_{\text{op}}(E, \hat{E}) \\ & = \epsilon, \end{aligned} \quad (23)$$

since  $d_{\text{op}}$  satisfies triangle inequality and

$$d_{\text{op}}(\hat{E}, E^*) = \min_{Z \in \text{POVM}} d_{\text{op}}(\hat{E}, Z) \leq d_{\text{op}}(\hat{E}, E). \quad (24)$$

Then the theorem follows.  $\square$

Projecting  $\hat{E}$  onto the set of POVMs using  $d_{\text{op}}$  may become computationally demanding when  $L$  is large. As a practical alternative, one can perform the projection using any distance that upper bounds  $d_{\text{op}}$  [9, 31]. A natural choice is  $d_\infty = \min_{Z \in \text{POVM}} \sum_{i=1}^L \|\hat{E}_i - Z_i\|$ . Then,

$$d_{\text{op}}(\hat{E}, E_\infty^*) \leq d_{\text{op}}(E, \hat{E}) + d_{\text{op}}(\hat{E}, E^*) \quad (25)$$

$$\leq \frac{\epsilon}{2} + d_\infty. \quad (26)$$

$d_\infty$  can be calculated after the protocol is run, and in practice is of the order of  $\epsilon/2$ .

### C. Error analysis for average distance $d_{\text{av}}$

A similar calculation can be done to bound the error in the average distance  $d_{\text{av}}$ :

**Theorem 4.** Assume a POVM  $E$  acting on a Hilbert space dimension  $d$  and an IC set of states  $\{|\psi_i\rangle\}_{i=1}^M$ . To achieve a reconstruction error  $d_{\text{av}}(E, E^*) \leq \epsilon$  with probability  $1-\delta$  using the protocol described above, the required sample size is

$$N \geq \frac{8L^2(d^2 + d(1+\epsilon/3L))}{\epsilon^2} \ln\left(\frac{4Ld}{\delta}\right) \quad (27)$$

if  $\{|\psi_i\rangle\}_{i=1}^M$  is a 2-design and

$$N \geq \frac{8L^2(5^n + 2^n\epsilon/6)}{\epsilon^2} \ln\left(\frac{4L2^n}{\delta}\right). \quad (28)$$

if the POVM acts on an  $n$ -qubit system and  $\{|\psi_i\rangle\}_{i=1}^M$  is a tensor product of single-qubit 2-designs.

These sample complexity guarantees scale as order  $\mathcal{O}(d^2L^2/\epsilon^2)$  in the global 2-design setting, and as  $\mathcal{O}(L^2d^{2.33}/\epsilon^2)$  when using local 2-designs. Compared to the worst-case (operational) distance, this represents a reduction in sample complexity by a factor of  $d$ , but at the cost of an extra factor of  $L$ . This arises from applying the union bound over a sum, in contrast to the maximum used in the operational distance. Notice that for POVMs composed of rank-one projectors, where  $L = d$ , both average- and worst-case distances require a sample size  $\mathcal{O}(d^4/\epsilon^2)$ .

*Proof.* We start by bounding  $d_{\text{av}}(E, \hat{E})$  by  $\epsilon/2$ . Notice that

$$d_{\text{av}}(E, \hat{E}) \leq \frac{1}{2d} \sum_{i=1}^L \|E_i - \hat{E}_i\|_F + \left| \text{tr}(E_i - \hat{E}_i) \right|. \quad (29)$$

Bounding each of the terms on the right-hand side of Eq. (29) provides a bound for  $d_{\text{av}}(E, \hat{E})$ . We begin by bounding the first term by  $\frac{\epsilon}{4}$ . Recall that  $\|\cdot\|_F \leq \sqrt{d}\|\cdot\|$ . Using Eq. (18) for the global 2-design with  $x = \{j\}$  and  $t = \frac{\sqrt{d}\epsilon}{2L}$ , we have

$$\begin{aligned} \Pr\left(\frac{1}{2d} \|\hat{E}_j - E_j\|_F \geq \frac{\epsilon}{4L}\right) & \leq \Pr\left(\|\hat{E}_j - E_j\| \geq \frac{\sqrt{d}\epsilon}{2L}\right) \\ & \leq \frac{\delta}{2L}, \end{aligned} \quad (30)$$

where  $\delta/2L = 2d \exp\left(-\frac{N\epsilon^2/8L^2}{d^2+d(1+\epsilon\sqrt{d}/6L)}\right)$ . Using the union bound, we obtain

$$\Pr\left(\frac{1}{2d} \sum_{j=1}^L \|\hat{E}_j - E_j\|_F \geq \frac{\epsilon}{4}\right) \leq \delta/2. \quad (31)$$



This in turns implies that

$$N \geq \frac{8L^2(d^2 + d(1 + \sqrt{d\epsilon/6L}))}{\epsilon^2} \ln \left( \frac{4Ld}{\delta} \right). \quad (32)$$

To bound  $\frac{1}{2d} \sum_{i=1}^L |\text{tr}(E_i - \hat{E}_i)|$  we use Hoeffding's inequality. Note that  $\text{tr}(\hat{E}_i) = \frac{1}{N} \sum_{k=1}^N \text{tr}(\hat{X}_k)$ . Since  $\text{tr}(\hat{X}_k)$  is either  $d$  or  $0$ , we have

$$\begin{aligned} \Pr \left( \frac{1}{2d} \left| \text{tr}(E_i - \hat{E}_i) \right| \geq \frac{\epsilon}{4L} \right) &\leq 2 \exp(-\epsilon^2 N / 2L^2) \\ &= \frac{\delta}{2L}. \end{aligned} \quad (33)$$

Then, by the union bound,

$$\begin{aligned} \Pr \left( \frac{1}{2d} \sum_{i=1}^L \left| \text{tr}(E_i - \hat{E}_i) \right| \geq \frac{\epsilon}{4} \right) &\leq 2 \sum_{i=1}^L \exp(-\epsilon^2 N / 2L^2) \\ &= \delta/2. \end{aligned} \quad (34)$$

Thus, to ensure that  $\frac{1}{2d} \sum_{i=1}^L |\text{tr}(E_i - \hat{E}_i)| \leq \epsilon/4$  with probability at least  $1 - \delta/2$ , it suffices to have

$$N \geq \frac{2L^2}{\epsilon^2} \ln \left( \frac{4L}{\delta} \right). \quad (35)$$

Then, if we want an error  $d_{\text{av}}(E, \hat{E})$  smaller than  $\epsilon/2$  with probability  $1 - \delta$  using global 2-designs, we need

$$N \geq \frac{8L^2(d^2 + d(1 + \sqrt{d\epsilon/6L}))}{\epsilon^2} \ln \left( \frac{4Ld}{\delta} \right). \quad (36)$$

The bound  $d_{\text{av}}(E, E^*) \leq \epsilon$  follows by the same argument that we used in the bounds for  $d_{\text{op}}(E, E^*)$ . The bound for  $d_{\text{av}}(E, E^*)$  using local 2-designs can be found similarly.  $\square$

#### IV. MINIMUM SAMPLE COMPLEXITY

Here, we provide a lower bound for the sample complexity of non-adaptive measurement tomography considering the worst-case distance  $d_{\text{op}}$ . The proof is based on a discretization of the problem which allows us to relate quantum measurement tomography to the problem of discrimination of well-separated POVMs. We first construct a set of  $R \in \exp(\Omega(d^2))$  POVMs on dimension  $d$  that are  $\epsilon/8$  apart in operational distance from each other. We then encode a random message using this set and decode it using measurement tomography with sufficient precision. From Fano's inequality, this gives us a lower bound  $\Omega(d^2)$  for the mutual information between the encoder and decoder. Additionally, we obtain an upper bound  $\mathcal{O}(N\epsilon^2/d)$  for the mutual information between the parties after  $n$  uses of the POVM. Using these two results, we derive a bound  $N \geq \Omega(d^3/\epsilon^2)$  for the sample complexity of any non-adaptive tomographic procedure. These techniques have been previously employed in quantum information theory and are standard tools in the statistical estimation literature [13, 18, 32–35].

#### A. Construction of an $\epsilon$ -packing

Here, we will demonstrate the existence of a set of  $R \in \exp(\Omega(d^2))$  POVMs that are at least  $\epsilon/8$  apart in operational distance. Each POVM  $E_{U_x}$  in this set has  $L + 2$  elements of the form

$$\begin{aligned} E_{U_x}^k &= \frac{1}{2L} \mathbb{1} \quad \text{for } k = 1, \dots, L \\ E_{U_x}^{L+1} &= \frac{(1+\epsilon)}{4} \mathbb{1} - \frac{\epsilon}{2} U_x P U_x^\dagger \\ E_{U_x}^{L+2} &= \frac{(1-\epsilon)}{4} \mathbb{1} + \frac{\epsilon}{2} U_x P U_x^\dagger, \end{aligned} \quad (37)$$

where  $U_x$  is a unitary operator,  $P$  a projector of rank  $d/2$  and  $0 \leq \epsilon \leq 1/2$ .

To construct this packing, we require the following set of unitaries [18]:

**Lemma 5.** *There exists a set of  $R \in \exp(\Omega(d^2))$  unitaries such that for any  $U_i \neq U_j$  in the set,*

$$\frac{1}{d} \|U_i P U_i^\dagger - U_j P U_j^\dagger\|_1 \geq \frac{1}{4}, \quad (38)$$

where  $P$  is a fixed projector of rank  $d/2$ .

We will use this to prove the following

**Lemma 6.** *There exists a set of  $R \in \exp(\Omega(d^2))$  POVMs that are  $\epsilon/8$  apart in operational distance  $d_{\text{op}}$  from each other.*

*Proof.* From Lemma 5 we fix a set of  $R \in \exp(\Omega(d^2))$  unitaries to construct a set of POVMs in  $\exp(\Omega(d^2))$  of the form of Eq. (37). Then all the POVMs are at least  $\epsilon/8$  apart from each other:

$$\begin{aligned} d_{\text{op}}(E_{U_i}, E_{U_j}) &= \frac{\epsilon}{2} \|U_i P U_i^\dagger - U_j P U_j^\dagger\| \\ &\geq \frac{\epsilon}{2d} \|U_i P U_i^\dagger - U_j P U_j^\dagger\|_1 \\ &\geq \frac{\epsilon}{8}. \end{aligned} \quad (39)$$

$\square$

In the proof of the lower bound on the sample complexity, each POVM  $E_{U_x}$  of the form of Eq. (37) will encode a uniform random message  $X$  that will be decoded using the information given by the measurement outcomes  $Y$ .

#### B. Upper bound on mutual information

To prove the upper bound for the mutual information, we will first bound it in terms of the  $\chi^2$ -divergence [18]:

**Lemma 7.** *Let  $X$  be an arbitrary random variable and  $Z$  a discrete random variable. Then,*

$$I(X : Z) \leq \frac{1}{\ln(2)} \left( \sum_z \mathbb{E}_{X \sim p_X} \frac{p_{Z|X}(z)^2}{p_Z(z)} - 1 \right), \quad (40)$$

where  $p_Z$  is the probability distribution of  $Z$  and  $p_{Z|X}$  is the probability distribution of  $Z$  conditioned on the event  $X = x$ .

Measuring a set of states  $\{\rho_i\}_{i=1}^N$  using a random POVM  $E_{U_X}$  in our set of POVMs defines a random variable  $Y = (Y_1, \dots, Y_N)$  such that the probability of outcome  $y_i \in [L+2]$  in round  $i$  is given by  $p(Y_i = y_i) = \text{tr}(E_{U_X}^{y_i} \rho_i)$ . Computing the mutual information  $I(X : Y)$  is challenging because we do not have an explicit description of the POVMs in our construction. The next result, adapted from Proposition 4.3 in Ref. [18], allows us to replace our specific ensemble of POVMs with one defined using Haar-random unitaries in the analysis of mutual information:

**Lemma 8.** *Let  $X \sim \text{Unif}[R]$ ,  $U$  be a Haar random unitary and  $\{\rho_i\}_{i=1}^N$  a set of  $N$  quantum states. Then, there exists a set of  $R \in \exp(\Omega(d^2))$  POVMs of the form of Eq. (37) which forms an  $\epsilon/8$  packing and satisfies*

$$I(X : Y) \leq I(U : Z), \quad (41)$$

where  $Y = (Y_1, \dots, Y_N)$  is the outcome of measuring  $\{\rho_i\}_{i=1}^N$  with a random POVM  $E_{U_X}$  and  $Z = (Z_1, \dots, Z_N)$  is the outcome of measuring  $\{\rho_i\}_{i=1}^N$  with a random POVM  $E_U$ .

This result allows us to upper bound the mutual information by averaging over Haar-random unitaries, instead of computing it directly from the specific set of unitaries used in the  $\epsilon/8$ -packing.

Using these results and following Ref. [18] we obtain an upper bound for the mutual information:

**Lemma 9.** *Let  $X \sim \text{Unif}([R])$  and  $Y = (Y_1, Y_2, \dots, Y_N)$  be the outcome of the measurement of a random POVM  $E_{U_X}$  of the form of Eq. (37) over  $N$  quantum states. Then,*

$$I(X : Y) \leq \frac{N}{2 \ln(2)} \frac{\epsilon^2}{(d+1)} \quad (42)$$

*Proof.* We have

$$\begin{aligned} I(X : Y) &\leq I(U : Z) \\ &= \sum_{i=1}^N I(U : Z_i | Z_{i-1}, \dots, Z_1) \\ &\leq \sum_{i=1}^N I(U : Z_i) \\ &\leq \frac{N}{\ln(2)} \mathbb{E}_{U \sim \text{Haar}} \left( \sum_{z_i} \frac{p_{Z_i|U}(z_i)^2}{p_{Z_i}(z_i)} - 1 \right), \end{aligned} \quad (43)$$

where the first line follows from Lemma 8, the second one from the chain rule for mutual information, the third one from the independence of  $Z_1, \dots, Z_N$  given  $U$  and the final one from Lemma 7. Then, we have to calculate the values of  $p_{Z_i}(z_i)$  and  $\mathbb{E}_U p_{Z_i|U}(z_i)^2$ .

For POVM elements  $L+1$  and  $L+2$ , the probability  $p_{Z_i}(z_i) = \mathbb{E}_U p_{Z_i|U}(z_i)$  is of the form

$$p_{Z_i}(z_i) = \mathbb{E}_U \text{tr} \left( \left( \frac{(1 \pm \epsilon)}{4} \mathbf{1} \mp \frac{\epsilon}{2} U P U^\dagger \right) \rho \right) = \frac{1}{4}. \quad (44)$$

For  $i = 1 \dots L$  we have  $p_{Z_i}(z_i) = 1/(2L)$ . Next, we have for POVM elements  $L+1$  and  $L+2$ :

$$\begin{aligned} \mathbb{E}_U p_{Z_i|U}(z_i)^2 &= \mathbb{E}_U \text{tr} \left( \left( \frac{(1 \pm \epsilon)}{4} \mathbf{1} \mp \frac{\epsilon}{2} U P U^\dagger \right) \rho \right)^2 \\ &= \frac{1}{16} \left( 1 + \frac{\epsilon^2}{(d+1)} \right) \end{aligned} \quad (45)$$

and for  $i = 1 \dots L$  we have  $p_{Z_i}(z_i)^2 = 1/(4L^2)$ . Then, collecting these results and substituting in Eq. (43), we obtain

$$\begin{aligned} I(X : Y) &\leq \frac{N}{\ln(2)} \left( \sum_{z_i=1}^L \frac{1}{2L} + \frac{1}{2} \left( 1 + \frac{\epsilon^2}{(d+1)} \right) - 1 \right) \\ &= \frac{N}{2 \ln(2)} \frac{\epsilon^2}{(d+1)} \end{aligned} \quad (46)$$

□

### C. Lower bound on the sample complexity

Now we show a lower bound on the sample complexity

**Theorem 10.** *Any procedure for quantum measurement tomography of a POVM on a  $d$ -dimensional Hilbert space that is  $\epsilon/16$  accurate in operational distance using nonadaptive, single-copy measurements on known input states requires*

$$N \in \Omega \left( \frac{d^3}{\epsilon^2} \right) \quad (47)$$

*uses of the unknown POVM.*

*Proof.* Assume a random message is encoded in  $N$  copies of a POVM  $E_{U_X}$ , where this POVM is uniformly sampled from the  $\epsilon/8$ -packing defined by Lemma 6. Let  $Y = (Y_1, \dots, Y_N)$  denote the outcomes from measuring  $N$  known quantum states using the POVM. Since each POVM in the packing is separated by at least  $\epsilon/8$ , a tomography algorithm that takes this data and produces an estimate of the POVM within  $\epsilon/16$  precision in  $d_{\text{op}}$  (with some constant probability) is sufficient to decode the message. Then, tomography must have a sample complexity at least as large as the communication problem. From Lemma 9, the mutual information between the measurements used for tomography and the message is upper bounded by

$$I(X : Y) \leq \frac{N}{2 \ln(2)} \frac{\epsilon^2}{(d+1)}. \quad (48)$$

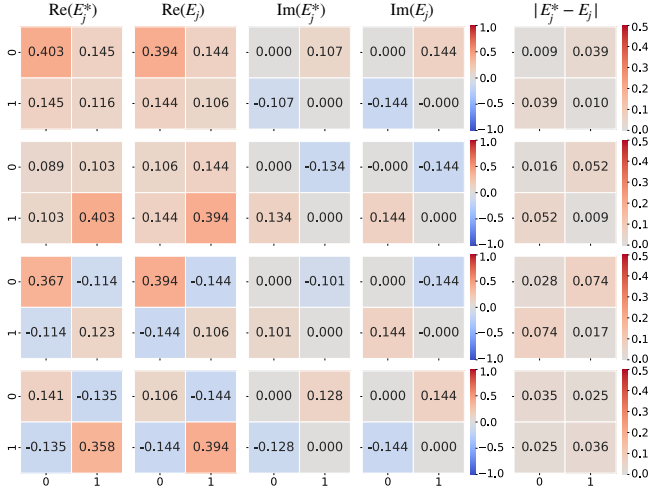


FIG. 2. Results for the reconstruction of a noisy one-qubit Symmetrical Informationally Complete (SIC-)POVM using an auxiliary qubit for the generalized measurement, implemented on a two-qubit flux-tunable transmon device using a budget of  $1.66 \cdot 10^5$  random initial states. The reconstructed noisy POVM is compared to its expected noiseless counterpart, with the absolute difference displayed. Though noisy, the reconstruction follows the target POVM closely. The deviations from the expected values are due to the noisy device implementation.

Using Lemma 2, we also have

$$I(X : Y) \geq \Omega(d^2). \quad (49)$$

Combining these results, we obtain

$$\frac{N}{2 \ln(2)} \frac{\epsilon^2}{(d+1)} \geq I(X : Y) \geq \Omega(d^2). \quad (50)$$

Thus, we conclude that

$$N \geq \Omega\left(\frac{d^3}{\epsilon^2}\right). \quad (51)$$

This is tight in the dimension (up to logarithmic factors), but we miss the factor  $L$  that appears in least-squares tomography.  $\square$

With a similar proof it can be shown that

$$N \geq \Omega\left(\frac{d^2 L}{\epsilon^2}\right) \quad (52)$$

to obtain precision  $\epsilon$  in  $d_{\text{av}}$  (see Appendix C). Since  $d_{\text{av}} \leq d_{\text{op}}$ , the lower bound on the sample complexity for  $d_{\text{av}}$  also applies to  $d_{\text{op}}$ .

## V. EMPIRICAL PERFORMANCE EVALUATIONS

Here we complement our theoretical findings with empirical performance studies on real quantum hardware.

Target POVMs are prepared using noisy quantum gates and readout. Then, quantum measurement tomography is used to recover the POVM performed on the noisy device. In this section, we present POVMs recovered from a noisy experiment, we showcase the performance of the method in a real scenario and we discuss its potential applications.

The experiment is performed on two superconducting flux-tunable transmon qubits. The device is controlled via microwave-based arbitrary waveform generators orchestrated and calibrated by open-source middleware [36, 37]. For further details, we refer to App. D.

The experiment consists of a two-pronged approach, where data acquisition and analysis are performed separately. Random initial states are generated from the ensemble of single-qubit 2-designs. In this case, the eigenstates of the Pauli operators are used. After  $N$  random states are drawn, the outcome statistics of the chosen POVM are aggregated in a vector of relative frequencies  $\hat{f}$ . With the data collected, post-processing starts by a least-squares estimator of each element of the POVM. This estimate, however does not generally conform to the physical conditions of a POVM, therefore a projection is needed to obtain the physical object we are interested in.

We choose a set of representative POVMs to showcase the capabilities of the algorithm. In this section we present results on a single-qubit Symmetrical Informationally Complete (SIC-)POVM that has been realized using one additional auxiliary qubit [38, 39]. That is, the setup involves two qubits in total. Appendix E contains additional performance studies for the two qubit Identity, Hadamard, Bell and Haar random measurements, as well as details on the implementation of the SIC-POVM.

The reconstruction of the experimental SIC-POVM is shown in Fig. 2. This has been performed with a budget of  $N = 1.66 \cdot 10^5$  initial states, randomly sampled from a single qubit two-design. It is readily apparent how the experiment follows the desired POVM. We also notice that there is a non-negligible difference between the experimental and target results. This difference is considerably larger than the precision of the reconstruction algorithm. This discrepancy is due to the experimental setup having inherent error in the gate application and readout that our protocol is precise enough to characterize.

This estimated POVM can be used to construct, for example, the half-sided noisy measurement channel. This channel combines the noisy estimation of the POVM with the ideal one. It is computed by using the noisy and exact POVM reconstructions,  $\{E_j^*\}_{j=1}^L$  and  $\{E_j\}_{j=1}^L$  respectively, in

$$\mathcal{M}^* = \sum_{j=1}^L |E_j\rangle\langle E_j^*|. \quad (53)$$

Here the round bra-ket follows the standard Dirac notation with respect to the Hilbert-Schmidt inner product  $\langle A|B \rangle = \text{tr}[A^\dagger B]$  with  $A, B$  linear operators [40]. This



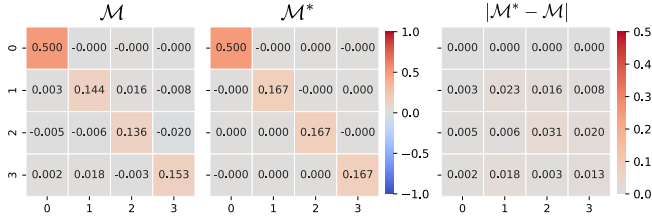


FIG. 3. Comparison of the half-sided noisy measurement channel with the expected channel for a one-qubit SIC-POVM. The channels are represented in Pauli basis. The absolute difference between them is also shown on the right. The half-sided noisy channel only slightly deviates from the expected results, proportional to the depolarizing channel. This reconstruction of the channel actually implemented in the device can be used to improve results executed on the experimental device.

half-sided measurement channel  $\mathcal{M}^*$  for the SIC-POVM is showed in Fig. 3, compared to the exact channel. We can see the effects of the noisy implementation on the recovered measurement channel. However, the difference between the expected and experimental results is small, and the proportionality to the effective depolarizing channel is still apparent. This channel is the key to error mitigation protocols for *classical shadows* [22, 35, 40–42]. More precisely, the classical shadow protocol [35] relies on the inversion of the measurement channel of a spherical two design, which is proportional to the effective depolarizing channel. Of course, when implementing this POVM measurements on a noisy device, the resulting channel will not be the expected one. Therefore, the mismatch of the implemented channel and the one inverted will introduce some error on the expectation values of interest. The presented protocol, however, can estimate the noisy experimental POVM, which can then be used in place of the depolarizing channel [41]. Several works have tackled this issue by estimating the noisy POVM implementation with different techniques [22, 40, 42], but our protocol offers both a practical and theoretical advancement on the previous methods, as it targets the noisy POVM implemented directly, making it a clear choice for the implementation of these robust classical shadow methods.

Furthermore, this protocol can be incorporated in calibration and characterization pipelines for quantum devices [22]. Understanding the error sources of these early devices is crucial to perform useful computations. These can be used to design error mitigation schemes and develop targeted error correction frameworks. Readout error is often decoupled from the rest of the process, our protocol instead provides a complete picture for complex measurements, that includes logical operations and auxiliary space.

## VI. SYNOPSIS

This work addresses the problem of quantum measurement tomography, which aims to reconstruct an unknown POVM based on the statistics obtained from a known set of input states. We propose and analyze a two-step reconstruction protocol that is both computationally fast and provably accurate. The protocol first constructs a linear least-squares estimator of the unknown POVM based on measurement statistics, and then projects this estimator onto the space of valid POVMs. This approach resembles projected least-squares quantum state and process tomography, but is adapted to the measurement problem [15, 16].

A key strength of our method is that the least-squares estimator can be computed analytically when the probe states are drawn from specific ensembles. We focus on two prominent choices: global unitary 2-designs and tensor products of local 2-designs. For both ensembles, we provide rigorous, non-asymptotic performance guarantees for our estimator in terms of its average-case and worst-case reconstruction error.

In particular, for a  $L$ -outcome POVM acting on a  $d$ -dimensional system, our method requires  $\mathcal{O}(d^3 L / \epsilon^2)$  samples to achieve error  $\epsilon$  in operational (worst-case) distance with high probability when using global 2-designs, and  $\mathcal{O}(d^{3.33} L / \epsilon^2)$  samples when using tensor products of single-qubit 2-designs. For average-case distance, the sample complexity is  $\mathcal{O}(d^2 L^2 / \epsilon^2)$  and  $\mathcal{O}(d^{2.33} L^2 / \epsilon^2)$ , respectively.

To assess the optimality of our approach, we also derive lower bounds on the sample complexity of any non-collective, non-adaptive QMT protocol. Our proof combines techniques from quantum information theory and classical statistics, such as discretization arguments and Fano’s inequality. We show that any protocol aiming to reconstruct an unknown POVM up to error  $\epsilon$  must use at least  $\Omega(d^3 / \epsilon^2)$  samples for the operational distance and  $\Omega(d^2 L / \epsilon^2)$  samples for the average distance. These bounds match the dimension scaling of our upper bounds up to logarithmic factors.

Still, a gap remains in the dependence on the number of POVM outcomes  $L$ . While our upper bounds scale linearly (or quadratically, in the average-case setting) in  $L$ , our current lower bounds miss that factor. Despite significant effort, we were unable to close this gap, and we leave the problem of establishing tight  $L$ -scaling bounds as an open question for future work.

Finally, we complement our theoretical results with empirical studies on actual quantum hardware. Our experiments validate the practical performance of our protocol and demonstrate its robustness under real noise conditions. Moreover, we discuss the usage of the protocol in the context of error mitigation and characterization of contemporary devices.

## ACKNOWLEDGMENTS

LZ was supported by the Government of Spain (Severo Ochoa CEX2019-000910-S, FUNQIP and European Union NextGenerationEU PRTR-C17.I1), Fundació Cellex, Fundació Mir-Puig, Generalitat de Catalunya (CERCA program), and the EU Quanterra project Veriq-

tas. SRC would like to acknowledge the calibration team at Technology Innovation Institute (TII) for assistance with the experimental setup. RK acknowledges financial support from the Austrian Science Fund (FWF) via the START award q-shadows (713361001) and the SFB BeyondC (10.55776/FG7) (research group 7).

- 
- [1] J. Fiurásek, Maximum-likelihood estimation of quantum measurement, *Phys. Rev. A* **64**, 024102 (2001).
  - [2] G. M. D'Ariano, L. Maccone, and P. L. Presti, Quantum calibration of measurement instrumentation, *Phys. Rev. Lett.* **93**, 250407 (2004).
  - [3] J. S. Lundeen, A. Feito, H. Coldenstrodt-Ronge, K. L. Pregnell, C. Silberhorn, T. C. Ralph, J. Eisert, M. B. Plenio, and I. A. Walmsley, Tomography of quantum detectors, *Nat. Phys.* **5**, 27 (2009).
  - [4] A. Feito, J. Lundeen, H. Coldenstrodt-Ronge, J. Eisert, M. B. Plenio, and I. A. Walmsley, Measuring measurement: theory and practice, *New J. Phys.* **11**, 093038 (2009).
  - [5] L. Zhang, A. Datta, H. B. Coldenstrodt-Ronge, X.-M. Jin, J. Eisert, M. B. Plenio, and I. A. Walmsley, Recursive quantum detector tomography, *New J. Phys.* **14**, 115005 (2012).
  - [6] Y. Chen, M. Farahzad, S. Yoo, and T.-C. Wei, Detector tomography on ibm quantum computers and mitigation of an imperfect measurement, *Phys. Rev. A* **100**, 052315 (2019).
  - [7] M. Cattaneo, M. A. Rossi, K. Korhonen, E.-M. Borelli, G. García-Pérez, Z. Zimborás, and D. Cavalcanti, Self-consistent quantum measurement tomography based on semidefinite programming, *Phys. Rev. Res.* **5**, 033154 (2023).
  - [8] S. Grandi, A. Zavatta, M. Bellini, and M. G. Paris, Experimental quantum tomography of a homodyne detector, *New J. Phys.* **19**, 053015 (2017).
  - [9] Y. Wang, S. Yokoyama, D. Dong, I. R. Petersen, E. H. Huntington, and H. Yonezawa, Two-stage estimation for quantum detector tomography: Error analysis, numerical and experimental results, *IEEE Trans. Inf. Theory* **67**, 2293 (2021).
  - [10] S. Xiao, Y. Wang, J. Zhang, D. Dong, S. Yokoyama, I. R. Petersen, and H. Yonezawa, On the regularization and optimization in quantum detector tomography, *Automatica* **155**, 111124 (2023).
  - [11] E. Nielsen, J. K. Gamble, K. Rudinger, T. Scholten, K. Young, and R. Blume-Kohout, Gate set tomography, *Quantum* **5**, 557 (2021).
  - [12] R. O'Donnell and J. Wright, Efficient quantum tomography, in *Proceedings of the Forty-Eighth Annual ACM Symposium on Theory of Computing*, STOC '16 (Association for Computing Machinery, New York, NY, USA, 2016) p. 899–912.
  - [13] J. Haah, A. W. Harrow, Z. Ji, X. Wu, and N. Yu, Sample-optimal tomography of quantum states, *IEEE Trans. Inf. Theory* **63**, 5628 (2017).
  - [14] R. Kueng, H. Rauhut, and U. Terstiege, Low rank matrix recovery from rank one measurements, *Appl. Comput. Harmon. Anal.* **42**, 88 (2017).
  - [15] M. Guță, J. Kahn, R. Kueng, and J. A. Tropp, Fast state tomography with optimal error bounds, *J. Phys. A: Math. Theor* **53**, 204001 (2020).
  - [16] T. Surawy-Stepney, J. Kahn, R. Kueng, and M. Guta, Projected least-squares quantum process tomography, *Quantum* **6**, 844 (2022).
  - [17] S. Chen, J. Li, B. Huang, and A. Liu, Tight bounds for quantum state certification with incoherent measurements, in *2022 IEEE 63rd Annual Symposium on Foundations of Computer Science (FOCS)* (IEEE, 2022) pp. 1205–1213.
  - [18] A. Lowe and A. Nayak, Lower bounds for learning quantum states with single-copy measurements, *arXiv:2207.14438* (2022).
  - [19] A. Anshu and S. Arunachalam, A survey on the complexity of learning quantum states, *Nat. Rev. Phys.* **6**, 59 (2024).
  - [20] M. Navascués and S. Popescu, How energy conservation limits our measurements, *Phys. Rev. Lett.* **112**, 140502 (2014).
  - [21] Z. Puchała, L. Paweł, A. Krawiec, and R. Kukulski, Strategies for optimal single-shot discrimination of quantum measurements, *Phys. Rev. A* **98**, 042103 (2018).
  - [22] F. B. Maciejewski, Z. Zimborás, and M. Oszmaniec, Mitigation of readout noise in near-term quantum devices by classical post-processing based on detector tomography, *Quantum* **4**, 257 (2020).
  - [23] F. B. Maciejewski, Z. Puchała, and M. Oszmaniec, Exploring quantum average-case distances: Proofs, properties, and examples, *IEEE Trans. Inf. Theory* **69**, 4600 (2023).
  - [24] R. Ahlswede and A. Winter, Strong converse for identification via quantum channels, *IEEE Trans. Inf. Theory* **48**, 569 (2002).
  - [25] J. A. Tropp, User-friendly tail bounds for sums of random matrices, *Found. Comput. Math.* **12**, 389 (2012).
  - [26] D. Gross, Recovering low-rank matrices from few coefficients in any basis, *IEEE Trans. Inf. Theory* **57**, 1548 (2011).
  - [27] R. Vershynin, *High-Dimensional Probability: An Introduction with Applications in Data Science* (Cambridge University Press, 2018).
  - [28] C. Dankert, R. Cleve, J. Emerson, and E. Livine, Exact and approximate unitary 2-designs and their application to fidelity estimation, *Phys. Rev. A* **80**, 012304 (2009).
  - [29] J. M. Renes, R. Blume-Kohout, A. J. Scott, and C. M. Caves, Symmetric informationally complete quantum measurements, *J. Math. Phys.* **45**, 2171 (2004).
  - [30] A. Klappenecker and M. Rotteler, Mutually unbiased bases are complex projective 2-designs, in *Proceedings. International Symposium on Information Theory, 2005. ISIT 2005.* (IEEE, 2005) pp. 1740–1744.

- [31] J. Barberà-Rodríguez, L. Zambrano, A. Acín, and D. Farina, Boosting projective methods for quantum process and detector tomography, [Physical Review Research \*\*7\*\*, 013208 \(2025\)](#).
- [32] J. Scarlett and V. Cevher, An introductory guide to fano's inequality with applications in statistical estimation, [arXiv:1901.00555 \(2019\)](#).
- [33] S. T. Flammia, D. Gross, Y.-K. Liu, and J. Eisert, Quantum tomography via compressed sensing: error bounds, sample complexity and efficient estimators, [New J. Phys. \*\*14\*\*, 095022 \(2012\)](#).
- [34] I. Roth, R. Kueng, S. Kimmel, Y.-K. Liu, D. Gross, J. Eisert, and M. Kliesch, Recovering quantum gates from few average gate fidelities, [Phys. Rev. Lett. \*\*121\*\*, 170502 \(2018\)](#).
- [35] H.-Y. Huang, R. Kueng, and J. Preskill, Predicting many properties of a quantum system from very few measurements, [Nat. Phys. \*\*16\*\*, 1050 \(2020\)](#).
- [36] S. Efthymiou, A. Orgaz-Fuertes, R. Carobene, J. Cereijo, A. Pasquale, S. Ramos-Calderer, S. Bordoni, D. Fuentes-Ruiz, A. Candido, E. Pedicillo, *et al.*, Qibolab: an open-source hybrid quantum operating system, [Quantum \*\*8\*\*, 1247 \(2024\)](#).
- [37] A. Pasquale, E. Pedicillo, J. Cereijo, S. Ramos-Calderer, A. Candido, G. Palazzo, R. Carobene, M. Gobbo, S. Efthymiou, Y. P. Tan, *et al.*, Qibocal: an open-source framework for calibration of self-hosted quantum devices, [arXiv:2410.00101 \(2024\)](#).
- [38] Z. Jiang, A. Kalev, W. Mruczkiewicz, and H. Neven, Optimal fermion-to-qubit mapping via ternary trees with applications to reduced quantum states learning, [Quantum \*\*4\*\*, 276 \(2020\)](#).
- [39] Z. You, Q. Liu, and Y. Zhou, Circuit optimization of qubit ic-povms for shadow estimation, [arXiv:2409.05676 \(2024\)](#).
- [40] R. Brieger, I. Roth, and M. Kliesch, Compressive gate set tomography, [PRX Quantum \*\*4\*\*, 010325 \(2023\)](#).
- [41] S. Chen, W. Yu, P. Zeng, and S. T. Flammia, Robust shadow estimation, [PRX Quantum \*\*2\*\*, 030348 \(2021\)](#).
- [42] E. Van Den Berg, Z. K. Mineev, and K. Temme, Model-free readout-error mitigation for quantum expectation values, [Phys. Rev. A \*\*105\*\*, 032620 \(2022\)](#).
- [43] E. Meckes and M. Meckes, Spectral measures of powers of random matrices, [ECP \*\*18\*\*, 1 \(2013\)](#).

## Appendix A: Estimator using 2-designs

### 1. Least-squares estimator using 2-designs

The measurement step in the protocol defines a linear map  $\mathcal{M} : M(\mathbb{C}^d) \rightarrow \mathbb{R}^M$  from POVM elements to probabilities. The map is defined as

$$[\mathcal{M}(X)]_i = \frac{1}{M} \langle \psi_i | X | \psi_i \rangle, \quad (\text{A1})$$

where  $\{|\psi_i\rangle\}_{i=1}^M$  is a set of states that forms a 2-design. In the experiment, we uniformly sample a state from the set, prepare it, and then measure it using a POVM  $E$  with elements  $(E_1, E_2, \dots, E_L)$ . After performing several rounds of this procedure, the collected data consists of a vector of relative frequencies  $\hat{f} \in \mathbb{R}^{M \times L}$ , where  $\hat{f}_{ij}$  is the relative frequency corresponding to the outcome  $j$  when measuring state  $|\psi_i\rangle$ . The relation between the frequencies and the POVM elements is given by

$$\hat{f}_j = \mathcal{M}(E_j) + \varepsilon, \quad (\text{A2})$$

where  $\hat{f}_j = (\hat{f}_{1j}, \hat{f}_{2j}, \dots, \hat{f}_{Mj})$  are all the frequencies associated to  $E_j$  and  $\varepsilon$  represents statistical noise due to the finite sample size.

The task of POVM estimation can be formulated as a least-squares problem. The goal is to find estimators  $\hat{E}_j$  that minimize the difference between the observed data  $\hat{f}_j$  and the model  $\mathcal{M}(E_j)$ . The least-squares solution is given by

$$\hat{E}_j = (\mathcal{M}^\dagger \mathcal{M})^{-1} (\mathcal{M}^\dagger (\hat{f}_j)), \quad (\text{A3})$$

where  $\mathcal{M}^\dagger : \mathbb{R}^M \rightarrow M(\mathbb{C}^d)$  is the adjoint map of  $\mathcal{M}$ .

To compute the solution, we leverage the 2-design property of the states  $\{|\psi_i\rangle\}_{i=1}^M$ . Specifically, it can be shown that the map  $\mathcal{M}^\dagger \mathcal{M}$  satisfies [15]

$$\begin{aligned} \mathcal{M}^\dagger \mathcal{M}(X) &= \frac{1}{M^2} \sum_{i=1}^M \langle \psi_i | X | \psi_i \rangle |\psi_i\rangle \langle \psi_i| \\ &= \frac{X + \text{tr}(X) \mathbb{1}}{d(d+1)M}. \end{aligned} \quad (\text{A4})$$

This result simplifies the inversion of  $\mathcal{M}^\dagger \mathcal{M}$ . The inverse channel is given by

$$(\mathcal{M}^\dagger \mathcal{M})^{-1}(X) = dM((d+1)X - \text{tr}(X)\mathbb{1}). \quad (\text{A5})$$

Substituting this into the least-squares solution, (A3), we find that the estimators  $\hat{E}_j$  take the form

$$\begin{aligned} \hat{E}_j &= (\mathcal{M}^\dagger \mathcal{M})^{-1} (\mathcal{M}^\dagger (\hat{f}_j)) \\ &= (\mathcal{M}^\dagger \mathcal{M})^{-1} \left( \frac{1}{M} \sum_{i=1}^M \hat{f}_{ij} |\psi_i\rangle \langle \psi_i| \right) \\ &= \sum_{i=1}^M \hat{f}_{ij} (d(d+1) |\psi_i\rangle \langle \psi_i| - d\mathbb{1}). \end{aligned} \quad (\text{A6})$$

Thus, the least-squares estimator provides a closed-form reconstruction of the POVM elements from the observed data.

### 2. Parameters for matrix Bernstein inequality using 2-designs

Now we want to bound the error in the protocol. For the matrix Bernstein inequality, Eq. (5), we need to calculate the parameters  $K$  and  $\sigma$  for the random matrices  $\frac{1}{N} (\hat{X}_k^{(x)} - F^{(x)})$ , where  $F^{(x)}$  is a POVM element that groups the outcomes  $j \in x$  and  $\hat{X}_k = d(d+1) |\psi_i\rangle \langle \psi_i| - d\mathbb{1}$  with probability  $p_i = \frac{1}{M} \langle \psi_i | F^{(x)} | \psi_i \rangle$  and zero with probability  $1 - \sum_i p_i$ . Since all the  $\hat{X}_k$  are i.i.d, for  $K$  we have

$$\begin{aligned} K &= \frac{1}{N} \left\| \left( \hat{X} - F \right) \right\| \\ &\leq \frac{1}{N} \max\{\|\hat{X}\|, \|F\|\} \\ &\leq \max_{i \in [M]} \frac{1}{N} \|d(d+1) |\psi_i\rangle \langle \psi_i| - d\mathbb{1}\| \\ &\leq \frac{d^2}{N}. \end{aligned} \quad (\text{A7})$$

For the variance, we have to calculate

$$\sigma^2 = \frac{1}{N^2} \left\| \sum_{k=1}^N \mathbb{E} [\hat{X}_k^2] - \left( F^{(x)} \right)^2 \right\|. \quad (\text{A8})$$

Here

$$\begin{aligned} \mathbb{E} [\hat{X}^2] &= \sum_{i=1}^M \frac{1}{M} \langle \psi_i | F | \psi_i \rangle \nu_i^2 \\ &= \sum_{i=1}^M \frac{1}{M} \langle \psi_i | F | \psi_i \rangle (d(d-1)\nu_i + d^3\mathbb{1}) \\ &= d(d-1)F + d^3 \sum_{i=1}^M \frac{1}{M} \langle \psi_i | F | \psi_i \rangle \mathbb{1} \\ &= d(d-1)F + d^2 \text{tr}(F) \mathbb{1}, \end{aligned} \quad (\text{A9})$$

since  $\{\frac{d}{M} |\psi_i\rangle \langle \psi_i|\}_{i=1}^M$  forms a POVM and then  $d \sum_{i=1}^M \frac{1}{M} \langle \psi_i | F | \psi_i \rangle = \text{tr}(F) \leq d$ . From these results we obtain

$$\begin{aligned} \sigma^2 &= \frac{1}{N} \|d(d-1)F + d^2 \text{tr}(F) \mathbb{1} - F\| \\ &\leq \frac{d^2(d+1)}{N}. \end{aligned} \quad (\text{A10})$$

## Appendix B: Estimator using single-qubit 2-designs

### 1. Least-squares estimator using single-qubit 2-designs

We now assume we have an  $n$ -qubit system and that the set of states  $\{|\psi_i\rangle\}_{i=1}^M$  we measure is a tensor product of  $n$  single-qubit sets  $\{|\psi_{i_k}\rangle\}_{i_k=1}^m$  that form a 2-design. Then, we have  $M = m^n$  elements of the form

$$|\psi_i\rangle = |\psi_{i_1}\psi_{i_2}\dots\psi_{i_n}\rangle, \quad (\text{B1})$$

Since for each qubit we have a local 2-design, we can define reduced channels  $\mathcal{M}_k : M(\mathbb{C}^2) \rightarrow \mathbb{R}^m$  for each qubit  $k$ . Then, the map  $\mathcal{M}_k^\dagger \mathcal{M}_k$  can be calculated as

$$\mathcal{M}_k^\dagger \mathcal{M}_k(X) = \frac{X + \text{tr}(X)\mathbb{1}}{6m}, \quad (\text{B2})$$

with inverse

$$\left(\mathcal{M}_k^\dagger \mathcal{M}_k\right)^{-1}(X) = 2m(3X - \text{tr}(X)\mathbb{1}). \quad (\text{B3})$$

Following Ref. [15], the total channel is just a tensor product of the local channels,

$$\mathcal{M}^\dagger \mathcal{M}(X) = \bigotimes_{k=1}^n \frac{X + \text{tr}(X)\mathbb{1}}{6m} \quad (\text{B4})$$

with inverse

$$\begin{aligned} (\mathcal{M}^\dagger \mathcal{M})^{-1}(X) &= \bigotimes_{k=1}^n 2m(3X - \text{tr}(X)\mathbb{1}) \\ &= M \bigotimes_{k=1}^n (6X - 2\text{tr}(X)\mathbb{1}). \end{aligned} \quad (\text{B5})$$

Applying the formula for the least squares estimator, we obtain

$$\begin{aligned} \hat{E}_j &= (\mathcal{M}^\dagger \mathcal{M})^{-1} \left( \mathcal{M}^\dagger \left( \hat{f}_j \right) \right) \\ &= (\mathcal{M}^\dagger \mathcal{M})^{-1} \left( \frac{1}{M} \sum_{i=1}^M \hat{f}_{ij} |\psi_i\rangle \langle \psi_i| \right) \\ &= \sum_{i=1}^M \hat{f}_{ij} \bigotimes_{k=1}^n (6|\psi_{i_k}\rangle \langle \psi_{i_k}| - 2\mathbb{1}). \end{aligned} \quad (\text{B6})$$

### 2. Parameters for matrix Bernstein inequality using local 2-designs

For the matrix Bernstein inequality we need to calculate the parameters  $K$  and  $\sigma$  for the random matrices  $\frac{1}{N} \left( \hat{X}_k^{(x)} - F^{(x)} \right)$ , where  $F^{(x)}$  is a POVM element that groups the outcomes  $j \in x$  and  $\hat{X}_k = \bigotimes_{k=1}^n (6|\psi_{i_k}\rangle \langle \psi_{i_k}| - 2\mathbb{1})$  with probability  $p_i =$

$\frac{1}{M} \langle \psi_i | F^{(x)} | \psi_i \rangle$  and zero with probability  $1 - \sum_i p_i$ . Since all the  $\hat{X}_k$  are i.i.d., for  $K$  we have

$$\begin{aligned} K &= \frac{1}{N} \left\| \left( \hat{X} - F \right) \right\| \\ &\leq \frac{1}{N} \max \{ \|\hat{X}\|, \|F\| \} \\ &\leq \max_{i \in [M]} \frac{1}{N} \prod_{k=1}^n \|6|\psi_{i_k}\rangle \langle \psi_{i_k}| - 2\mathbb{1}\| \end{aligned} \quad (\text{B7})$$

$$\leq \frac{4^n}{N}. \quad (\text{B8})$$

The variance is given by

$$\sigma^2 = \frac{1}{N^2} \left\| \sum_{k=1}^N \mathbb{E} \left[ \hat{X}^2 \right] - \left( F^{(x)} \right)^2 \right\|. \quad (\text{B9})$$

Then, we need to calculate  $\mathbb{E} \left[ \hat{X}^2 \right]$ . Assuming the POVM is separable,  $F = \bigotimes_{k=1}^n F_k$ , we can decompose

$$\begin{aligned} &\frac{1}{M} \langle \psi_i | F | \psi_i \rangle \bigotimes_{k=1}^n (6|\psi_{i_k}\rangle \langle \psi_{i_k}| - 2\mathbb{1})^2 \\ &= \frac{1}{M} \bigotimes_{k=1}^n \langle \psi_{i_k} | F_k | \psi_{i_k} \rangle (6|\psi_{i_k}\rangle \langle \psi_{i_k}| - 2\mathbb{1})^2. \end{aligned} \quad (\text{B10})$$

Then,

$$\begin{aligned} \mathbb{E} \left[ \hat{X}^2 \right] &= \bigotimes_{k=1}^n \sum_{i_k=1}^m \frac{\langle \psi_{i_k} | F_k | \psi_{i_k} \rangle}{m} (6|\psi_{i_k}\rangle \langle \psi_{i_k}| - 2\mathbb{1})^2 \\ &= 2^n \bigotimes_{k=1}^n \sum_{i_k=1}^m \frac{\langle \psi_{i_k} | F_k | \psi_{i_k} \rangle}{m} (6|\psi_{i_k}\rangle \langle \psi_{i_k}| - 2\mathbb{1} + 4\mathbb{1}) \\ &= 2^n \bigotimes_{k=1}^n \left( F_k + 4 \sum_{i_k=1}^m \frac{\langle \psi_{i_k} | F_k | \psi_{i_k} \rangle}{m} \mathbb{1} \right) \\ &= 2^n \bigotimes_{k=1}^n (F_k + 2\text{tr}(F_k)\mathbb{1}) \\ &= 2^n \sum_{\alpha \subseteq \mathcal{P}(n)} 2^{|\alpha|} \text{tr}_\alpha(F) \otimes \mathbb{1}^{\otimes \alpha}, \end{aligned} \quad (\text{B11})$$

where  $\text{tr}_\alpha(F)$  is the trace of the elements with indices in  $\alpha$ . By linearity this is also true for any POVM element, and then, using that  $F \leq \mathbb{1}$ , we obtain [15]

$$\begin{aligned} \sigma^2 &\leq \frac{1}{N} \left\| \mathbb{E} \left[ \hat{X}^2 \right] \right\| \\ &\leq \frac{2^n}{N} \sum_{\alpha \subseteq \mathcal{P}(n)} 2^{|\alpha|} \|\text{tr}_\alpha(F)\| \\ &\leq \frac{2^n}{N} \sum_{\alpha \subseteq \mathcal{P}(n)} 2^{|\alpha|} \|\text{tr}_\alpha \mathbb{1}\| \\ &= \frac{2^n}{N} \sum_{\alpha \subseteq \mathcal{P}(n)} 4^{|\alpha|} \\ &= \frac{10^n}{N}. \end{aligned} \quad (\text{B12})$$



The last equality follows from  $\sum_{\alpha \subseteq \mathcal{P}(n)} 4^{|\alpha|} = \sum_{k=0}^n \binom{n}{k} 4^k = 5^n$ .

### Appendix C: Minimum sample complexity for $d_{\text{av}}$

Here, we provide a lower bound for the sample complexity of non-adaptive measurement tomography considering  $d_{\text{av}}$ . The proof is based on the discretization of the problem, reducing quantum measurement tomography to the problem of discrimination of well-separated POVMs. We first construct a set of  $R \in \exp(\Omega(d^2 L))$  POVMs on dimension  $d$  that are  $\epsilon/4$  apart in  $\sqrt{d} d_{\text{av}}$  from each other. We then encode a random message using this set and decode it using measurement tomography with sufficient precision. From Fano's inequality, this gives us a lower bound  $\Omega(d^2 L)$  for the mutual information between the encoder and decoder. Additionally, we obtain an upper bound  $\mathcal{O}(N\epsilon^2/d)$  for the mutual information between the parties after  $n$  uses of the POVM. Using these two results, we derive a bound  $N \geq \Omega(d^2 L/\epsilon^2)$  for the sample complexity of any non-adaptive tomographic procedure using  $d_{\text{av}}$ .

#### 1. Construction of an $\epsilon$ -packing

Let  $\{U_j\}_{j=1}^{L/2}$  be a set of Haar-random unitaries,  $P$  a rank- $d/2$  projector and  $E_{\{U_j\}}$  a POVM with  $L$  elements given by

$$\begin{aligned} E^j &= \frac{(1-\epsilon)}{L} \mathbb{1} + \frac{2\epsilon}{L} U_j P U_j^\dagger \\ E^{j+L/2} &= \frac{(1+\epsilon)}{L} \mathbb{1} - \frac{2\epsilon}{L} U_j P U_j^\dagger \end{aligned} \quad (\text{C1})$$

We want to construct a large set of POVMs of this form such that  $\sqrt{d} d_{\text{av}}(E_{\{U_j\}}, E_{\{V_j\}}) \geq \epsilon/4$ . To do this, we will use the following [43]:

**Theorem 11.** *Let  $k$  and  $d$  be positive integers and  $M = U_1(d) \times \dots \times U_k(d)$  a space equipped with the  $L_2$ -sum of Hilbert-Schmidt metrics. Suppose  $F : M \rightarrow \mathbb{R}$  is  $\kappa$ -Lipschitz, and that  $\{U_j \in U_j(d)\}$  are independent, Haar distributed unitary matrices. Then, for each  $t > 0$ ,*

$$\begin{aligned} \Pr(F(U_1, \dots, U_k) \geq \mathbb{E}[F(U_1, \dots, U_k)] + t) \\ \leq \exp\left(-\frac{dt^2}{12\kappa^2}\right). \end{aligned} \quad (\text{C2})$$

This theorem will give us a concentration inequality for  $d_{\text{av}}$ . Then, if we choose our set of POVMs randomly, it will be  $\epsilon$ -separated with high probability.

**Lemma 12.** *There exists a set of  $R \in \exp(\Omega(d^2 L))$  POVMs that are  $\epsilon/4$  apart in average distance  $d_{\text{av}}$  from each other.*

*Proof.* We want to use Theorem 11 for

$$\begin{aligned} F &= \frac{1}{2d} \sum_{i=1}^L \|E_{\{U_j\}}^i - E_{\{V_j\}}^i\|_F \\ &= \frac{\epsilon}{dL} \sum_{j=1}^L \|U_j P U_j^\dagger - V_j P V_j^\dagger\|_F, \end{aligned} \quad (\text{C3})$$

since this is a lower bound for  $d_{\text{av}}(E_{\{U_j\}}, E_{\{V_j\}})$ . Defining  $f_j = \|U_j P U_j^\dagger - V_j P V_j^\dagger\|_F$ , we need to calculate the Lipschitz constant  $\kappa$  (from the relation  $|F - F'| \leq \kappa \|(U_i, V_i) - (U'_i, V'_i)\|$ ) and  $\mathbb{E}\left[\frac{\epsilon}{dL} \sum_{j=1}^L f_j\right]$ . We start with the former. Using the reverse triangle inequality, we have

$$\begin{aligned} |f_j - f'_j| &\leq \|U_j P U_j^\dagger - V_j P V_j^\dagger - U'_j P U'_j{}^\dagger + V'_j P V'_j{}^\dagger\|_F \\ &\leq \|U_j P U_j^\dagger - U'_j P U'_j{}^\dagger\|_F + \|V_j P V_j^\dagger - V'_j P V'_j{}^\dagger\|_F. \end{aligned}$$

Then, since for unitaries  $W$  and  $W'$  we have the relation  $\|W_j P W_j^\dagger - W'_j P W'_j{}^\dagger\|_F \leq 2 \|W_j - W'_j\|_F$  and the unitaries satisfy  $W_j = W_{j+L/2}$  for  $j = 1, \dots, L/2$ , we obtain

$$\begin{aligned} \left| \sum_{j=1}^L f_j - f'_j \right| &\leq 4 \sum_{j=1}^{L/2} (\|U_j - U'_j\|_F + \|V_j - V'_j\|_F) \\ &\leq 4\sqrt{L} \left( \sum_{j=1}^{L/2} \|U_j - U'_j\|_F^2 + \|V_j - V'_j\|_F^2 \right)^{\frac{1}{2}}. \end{aligned} \quad (\text{C4})$$

This gives us an upper bound for the Lipschitz constant,  $\kappa \leq \frac{4\epsilon}{d\sqrt{L}}$ .

Now, we find a lower bound for the average  $\mathbb{E}\left[\frac{1}{L} \sum_{j=1}^L f_j\right]$  using [23]

$$\mathbb{E}_{U, V \sim \text{Haar}} f_j \geq \frac{(\mathbb{E}_{U, V} f_j^2)^{3/2}}{(\mathbb{E}_{U, V} f_j^4)^{1/2}}. \quad (\text{C5})$$

We have

$$\begin{aligned} \mathbb{E} f_j^2 &= \mathbb{E} \text{tr} \left( (U_j P U_j^\dagger - V_j P V_j^\dagger)^2 \right) \\ &= 2 \mathbb{E} \text{tr}(P^2) - 2 \mathbb{E} \text{tr}(U_j P U_j^\dagger V_j P V_j^\dagger) \\ &= 2 \left( \text{tr}(P^2) - \frac{\text{tr}(P)^2}{d} \right). \end{aligned} \quad (\text{C6})$$

Also,

$$\begin{aligned} \mathbb{E} f_j^4 &= 4 \mathbb{E} \left( \text{tr} \left( (U_j P U_j^\dagger - V_j P V_j^\dagger)^2 \right) \right)^2 \\ &= 4 \text{tr}(P^2)^2 - 8 \frac{\text{tr}(P^2) \text{tr}(P)^2}{d} \\ &\quad + 4 \frac{\text{tr}(P)^4 + \text{tr}(P^2)^2}{d^2 - 1} - 8 \frac{\text{tr}(P^2) \text{tr}(P)^2}{d(d^2 - 1)}. \end{aligned} \quad (\text{C7})$$

Since the projector  $P$  has rank  $d/2$ , we get

$$\mathbb{E} f_j^2 = \frac{d}{2}, \quad \mathbb{E} f_j^4 = \frac{d^4}{4(d^2 - 1)}. \quad (\text{C8})$$

This means that  $\mathbb{E} \left( \frac{\epsilon}{dL} \sum_{j=1}^L \|U_j P U_j^\dagger - V_j P V_j^\dagger\|_F \right) \geq \frac{\epsilon}{2\sqrt{d}}$ . Using Theorem 11, we have

$$\begin{aligned} & \Pr \left( \frac{\epsilon}{dL} \sum_{j=1}^L \|U_j P U_j^\dagger - V_j P V_j^\dagger\|_F \leq \frac{\epsilon}{4\sqrt{d}} \right) \\ & \leq \Pr \left( \frac{\epsilon}{2dL} \sum_{j=1}^L \|U_j P U_j^\dagger - V_j P V_j^\dagger\|_F - \frac{\epsilon}{2\sqrt{d}} \leq -\frac{\epsilon}{4\sqrt{d}} \right) \\ & \leq \exp \left( -\frac{d^2 L}{12 \times 64 \times 16} \right). \end{aligned} \quad (\text{C9})$$

Then, using probabilistic arguments, we can build a set of  $R \in \exp(-\Omega(d^2 L))$  POVMs

$$\begin{aligned} E^j &= \frac{(1-\epsilon)}{L} \mathbb{1} + \frac{2\epsilon}{L} U_j P U_j^\dagger \\ E^{j+L/2} &= \frac{(1+\epsilon)}{L} \mathbb{1} - \frac{2\epsilon}{L} U_j P U_j^\dagger \end{aligned} \quad (\text{C10})$$

that satisfy

$$\sqrt{d} d_{\text{av}}(E, F) \geq \frac{\epsilon}{4}. \quad (\text{C11})$$

□

## 2. Upper bound on mutual information for the average distance

**Lemma 13.** *Let  $X \sim \text{Unif}[R]$ ,  $\{U_j\}_{j=1}^{L/2}$  be a set of independent Haar random unitaries and  $\{\rho_i\}_{i=1}^N$  a set of  $N$  quantum states. Then, there exists a set of  $R \in \exp(\Omega(d^2 L))$  POVMs of the form of Eq. (C1) which forms an  $\epsilon/4$  packing for  $\sqrt{d} d_{\text{av}}$  and satisfies*

$$I(X : Y) \leq I(\{U_j\} : Z), \quad (\text{C12})$$

where  $Y = (Y_1, \dots, Y_N)$  is the outcome of measuring  $\{\rho_i\}_{i=1}^N$  with a random POVM  $E_{\{U_j^X\}}$  and  $Z = (Z_1, \dots, Z_N)$  is the outcome of measuring  $\{\rho_i\}_{i=1}^N$  with a random POVM  $E_{\{U_j\}}$ .

*Proof.* We closely follow Proposition 4.3 in Ref. [18]. Let  $X$  label a POVM of the form of Eq. (C1). The average distance for two POVMs of this form is invariant under the replacement  $U_j^X \rightarrow W_j U_j^X$  for arbitrary unitary operators  $\{W_j\}_{j=1}^{L/2}$ , since for two unitaries  $U$  and  $V$ , we have  $\|U P U^\dagger - V P V^\dagger\|_F = \|W U P U^\dagger W^\dagger - W V P V^\dagger W^\dagger\|_F$ . Then, this replacement maps an arbitrary initial  $\epsilon/4$ -packing to another one.

Define  $Y_W = (Y_1, \dots, Y_N)$ , with  $Y_i \in \{1, \dots, L\}$ , as the outcome random variable obtained by measuring the  $N$  copies  $\{\rho_i\}_{i=1}^N$  with  $E_{\{W_j U_j^X\}}$ . We claim that

$$\mathbb{E}_{\{W_j \sim \text{Haar}\}} I(X : Y_W) \leq I(\{U_j\} : Z) \quad (\text{C13})$$

for a set of independent, Haar distributed unitaries  $\{W_j\}_{j=1}^{L/2}$ . Let  $p_{Y|W,X}$  be the distribution of  $Y_W$  given  $\{U_j^X\}$ , with  $p_{Y|W,X}(Y = y) = \prod_{i=1}^N \text{tr}(E_{W_{y_i} U_{y_i}^X} \rho_i)$ . We have

$$\begin{aligned} \mathbb{E}_{\{W_j \sim \text{Haar}\}} I(X : Y_W) &= \mathbb{E}_{W_j} H \left( \mathbb{E}_{X \sim [R]} p_{Y|W,X} \right) \\ &\quad - \mathbb{E}_{W_j} \mathbb{E}_{X \sim [R]} H(p_{Y|W,X}) \\ &\leq H \left( \mathbb{E}_{X \sim [R]} \mathbb{E}_{W_j} p_{Y|W,X} \right) \\ &\quad - \mathbb{E}_{X \sim [R]} \mathbb{E}_{W_j} H(p_{Y|W,X}). \end{aligned} \quad (\text{C14})$$

The first line is just the definition of the mutual information, and the second one follows from the concavity of entropy. By the invariance of the Haar measure, we have that  $\mathbb{E}_{\{W_j \sim \text{Haar}\}} p_{Y|W,X} = \mathbb{E}_{\{W_j \sim \text{Haar}\}} p_{Y|W}$  and  $\mathbb{E}_{\{W_j \sim \text{Haar}\}} H(p_{Y|W,X}) = \mathbb{E}_{\{W_j \sim \text{Haar}\}} H(p_{Y|W})$ . The probability distribution of the outcomes of the random POVM  $E_{\{U_j\}}$  is defined as  $p_Z = \mathbb{E}_{\{U_j \sim \text{Haar}\}} p_{Y|U} = \mathbb{E}_{\{W_j \sim \text{Haar}\}} p_{Y|W}$ . Using Eq. (C14), this means that

$$\mathbb{E}_{\{W_j \sim \text{Haar}\}} I(X : Y_W) \leq I(\{U_j\} : Z). \quad (\text{C15})$$

Since the expectation of  $I(X : Y_W)$  over all sets of unitary operators  $\{W_j\}_{j=1}^{L/2}$  is at most  $I(\{U_j\} : Z)$ , there exists at least one set of unitary operators  $\{W_j\}_{j=1}^{L/2}$  for which the inequality  $I(X : Y_W) \leq I(\{U_j\} : Z)$  holds. Then we consider the set of POVMs  $\{E^{\{V_i U_i^X\}}\}$ . □

This means that in the calculation of the mutual information we can replace the average over the unitaries that define the  $\epsilon/4$ -packing by an average over Haar random unitaries to obtain an upper bound. This is given by [18]

**Lemma 14.** *Let  $X \sim \text{Unif}([R])$  and  $Y = (Y_1, Y_2, \dots, Y_N)$  be the outcome of the measurement of a random POVM  $E_{\{U_X\}}$  of the form of Eq. (C1) over  $N$  quantum states. Then,*

$$I(X : Y) \leq \frac{N}{\ln(2)} \frac{\epsilon^2}{(d+1)} \quad (\text{C16})$$

*Proof.* We have

$$I(X : Y) \leq I(\{U_j\} : Z) \quad (\text{C17})$$

$$= \sum_{i=1}^N I(\{U_j\} : Z_i | Z_{i-1}, \dots, Z_1) \quad (\text{C18})$$

$$\leq \sum_{i=1}^N I(\{U_j\} : Z_i) \quad (\text{C19})$$

$$\leq \frac{N}{\ln(2)} \mathbb{E}_{\{U_j\}} \left( \sum_{z_i} \frac{p_{Z_i|U_{z_i}}(z_i)^2}{p_{Z_i}(z_i)} - 1 \right), \quad (\text{C20})$$

where the first inequality follows from Lemma 13, the second one from the chain rule for mutual information, the third one from the independence of  $Z_1, \dots, Z_N$  given  $\{U_j\}$  and the final one from Lemma 14 and the independence of  $\{U_j\}$ .

The probability  $p_{Z_i}(z_i) = \mathbb{E}_{\{U_j\}} p_{Z_i|\{U_{z_i}\}}$  is of the form

$$\begin{aligned} p_{Z_i}(z_i) &= \mathbb{E}_{U_i \sim \text{Haar}} \text{tr} \left( \left( \frac{(1 \pm \epsilon)}{L} \mathbb{1} \mp \frac{2\epsilon}{L} U_i P U_i^\dagger \right) \rho \right) \\ &= \frac{1}{L} \end{aligned} \quad (\text{C21})$$

For the other term, we have

$$\begin{aligned} \mathbb{E}_{U_i \sim \text{Haar}} p_{Z_i|U_i}(z_i)^2 &= \mathbb{E}_{U_i} \text{tr} \left( \left( \frac{(1 \pm \epsilon)}{L} \mathbb{1} \mp \frac{2\epsilon}{L} U_i P U_i^\dagger \right) \rho \right)^2 \\ &= \frac{1}{L} \left( 1 + \frac{\epsilon^2}{(d+1)} \right). \end{aligned} \quad (\text{C22})$$

Then, using Lemma 7, we obtain

$$\begin{aligned} I(X : Y) &\leq \frac{N}{\ln(2)} \left( \sum_{z_i=1}^L \frac{1}{L} \left( 1 + \frac{\epsilon^2}{(d+1)} \right) - 1 \right) \\ &= \frac{N}{\ln(2)} \frac{\epsilon^2}{(d+1)}. \end{aligned} \quad (\text{C23})$$

□

### 3. Lower bound on the sample complexity of $d_{\text{av}}$

**Theorem 15.** *Any procedure for quantum measurement tomography of a POVM on a  $d$ -dimensional Hilbert space that is  $\epsilon/8$  accurate in average distance using nonadaptive, single-copy measurements on known input states requires*

$$N \in \Omega \left( \frac{d^2 L}{\epsilon^2} \right) \quad (\text{C24})$$

*uses of the unknown POVM.*

*Proof.* Similar to the calculation of the lower bound for  $d_{\text{op}}$ , assume a random message is encoded in  $N$  copies

of a POVM  $E_{\{U_j^x\}}$ , where this POVM is uniformly sampled from the  $\epsilon/4$ -packing defined by Lemma 12. Let  $Y = (Y_1, \dots, Y_N)$  denote the outcomes from measuring the random POVM over  $N$  quantum states. Since each POVM in the packing is separated by at least  $\epsilon/4$ , a tomography algorithm that takes this data and produces an estimate of the POVM within  $\epsilon/8$  precision in  $\sqrt{d} d_{\text{av}}$  (with some constant probability) is sufficient to decode the message. Then, tomography must have a sample complexity at least as large as the discrimination problem. From the previous section, the mutual information between the measurements used for tomography and the message is upper bounded by

$$I(X : Y) \leq \frac{N}{\ln(2)} \frac{\epsilon^2}{(d+1)}. \quad (\text{C25})$$

Using Lemma 2, we also have

$$I(X : Y) \geq \Omega(d^2). \quad (\text{C26})$$

Combining these results, we obtain

$$\frac{N}{\ln(2)} \frac{\epsilon^2}{(d+1)} \geq I(X : Y) \geq \Omega(d^2). \quad (\text{C27})$$

Thus, we conclude that

$$N \geq \Omega \left( \frac{d^3 L}{\epsilon^2} \right) \quad (\text{C28})$$

to obtain precision  $\epsilon$  in  $\sqrt{d} d_{\text{av}}$ . Then, to obtain precision  $\epsilon$  in  $d_{\text{av}}$ , we need at least

$$N \geq \Omega \left( \frac{d^2 L}{\epsilon^2} \right). \quad (\text{C29})$$

This matches the upper bound in the dimension  $d$ , but leaves a gap in the dependence on  $L$ . □

## Appendix D: Experimental details

The experiment is deployed on a subset of two connected qubits within a 5 qubit chip. It is a star topology flux-tunable superconducting transmon device manufactured by Quantware and hosted in the quantum computing lab of Technology Innovation Institute. The device is driven via microwave pulses generated via a Quantum Machines OPX system, orchestrated by the open source library Qibolab [36]. The system is calibrated using the available routines on the open source Qibocal [37] package.

The two qubits are calibrated up to usable specifications, as a reduced amount of noise is desirable for our presented algorithms to reconstruct the the noisy POVMs. The two qubits are calibrated before launching the experiment up to the following parameters: the relaxation times for the first and seconds qubits are

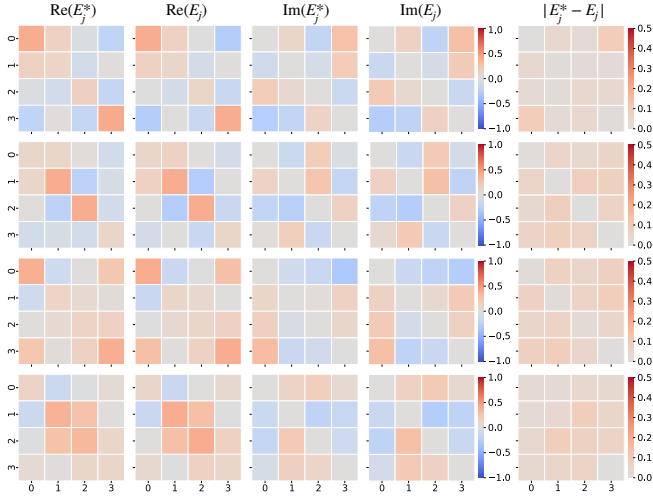


FIG. 4. Results for the reconstruction of the full system implementing a noisy two-qubit Symmetrical Informationally Complete (SIC-)POVM, implemented on a two-qubit flux-tunable transmon device using a budget of  $10^6$  random initial states. The reconstructed noisy POVM is compared to its expected noiseless counterpart, with the absolute difference displayed. Though noisy, the reconstruction follows the target POVM closely. The deviations from the expected values are due to the noisy device implementation.

$T_1^{(1)} = 33.6(6) \mu s$  and  $T_1^{(2)} = 30.6(6) \mu s$  respectively. Equally for the decoherence times  $T_2^{(1)} = 13.0(1) \mu s$  and  $T_2^{(2)} = 9.1(1) \mu s$ . Assignment fidelity for a computational basis readout of  $F_{ro}^{(1)} = 96.9(9) \%$  and  $F_{ro}^{(2)} = 98.0(0) \%$ . Lastly, the single qubit native pulse infidelity, as extracted from a randomized benchmarking experiment, of  $g_{inf}^{(1)} = 1.3(7) \cdot 10^{-3}$  and  $g_{inf}^{(2)} = 6.7(7) \cdot 10^{-3}$  for native pulse length of  $40 ns$ .

The experiments are designed directly in Qibolab language to leverage the lower level logic of the device. Everything is compiled down to the native pulses and interactions of the target quantum system. Code to reproduce the experiment is available upon reasonable request.

### Appendix E: Further results

Here we expand on the reconstruction of noisy experimental POVM implementation on a two-qubit supercon-

ducting flux-tunable transmon system. First we give details on the implementation of the SIC-POVM presented in the main text, such as circuits and further reconstructions. After, we present results on other POVMs, such as the Identity, a Hadamard gates or Haar random gates on both qubits, as well as a Bell measurement.

We create the SIC-POVM with a quantum circuit of the form shown in Fig. 5. The data qubit, where the initial state will be prepared is the second qubit in Fig. 5. The parameters for the single qubit rotations are taken as  $\theta = \arccos(1/\sqrt{3})$  and  $\phi = 3\pi/4$  [38] to generate a SIC-POVM [39]. Furthermore, we also characterize this POVM as a two-qubit measurement, instead of a projection into a single qubit system. In Fig. 4 we showcase the reconstruction. The results are similar to the ones in the main text, but in an extended space. Indeed, the single qubit POVM is located in the top left quadrant of the shown data.

In Fig 6 we collect all the data from the other POVM settings. First, on the top left are the results for the Identity POVM, that is, a direct measurement in the computational basis. While a very straight forward POVM, this reconstruction provides a great deal of information about the readout process of the device. For example, the non-symmetry in readout error when measuring different final states can be extracted from the data shown in this figure. On the top right, we plot the reconstruction results of a POVM measurement with a Hadamard gate before the readout, that is a measurement in the X basis — where we consider the usual convention of the computational basis being the Z direction. The bottom left graph shows a similar scenario, but with a single qubit Haar random gate before the readout. Unlike the other instances, in this one we notice how the reconstructed POVM is randomly spread across the real and imaginary space, without a directly apparent structure. At last, at the bottom right corner of Fig. 6 the results of the reconstruction of a noisy Bell POVM are shown.

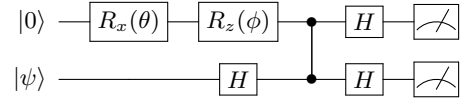


FIG. 5. Quantum circuit depicting the implementation of the SIC-POVM. When the single gate rotation parameters are  $\theta = \arccos(1/\sqrt{3})$  and  $\phi = 3\pi/4$ , this results in a Symmetrical Informationally Complete measurement. The choice of a CZ gate as the entangling operation is due to the native interactions of the experimental device where this protocol is deployed.

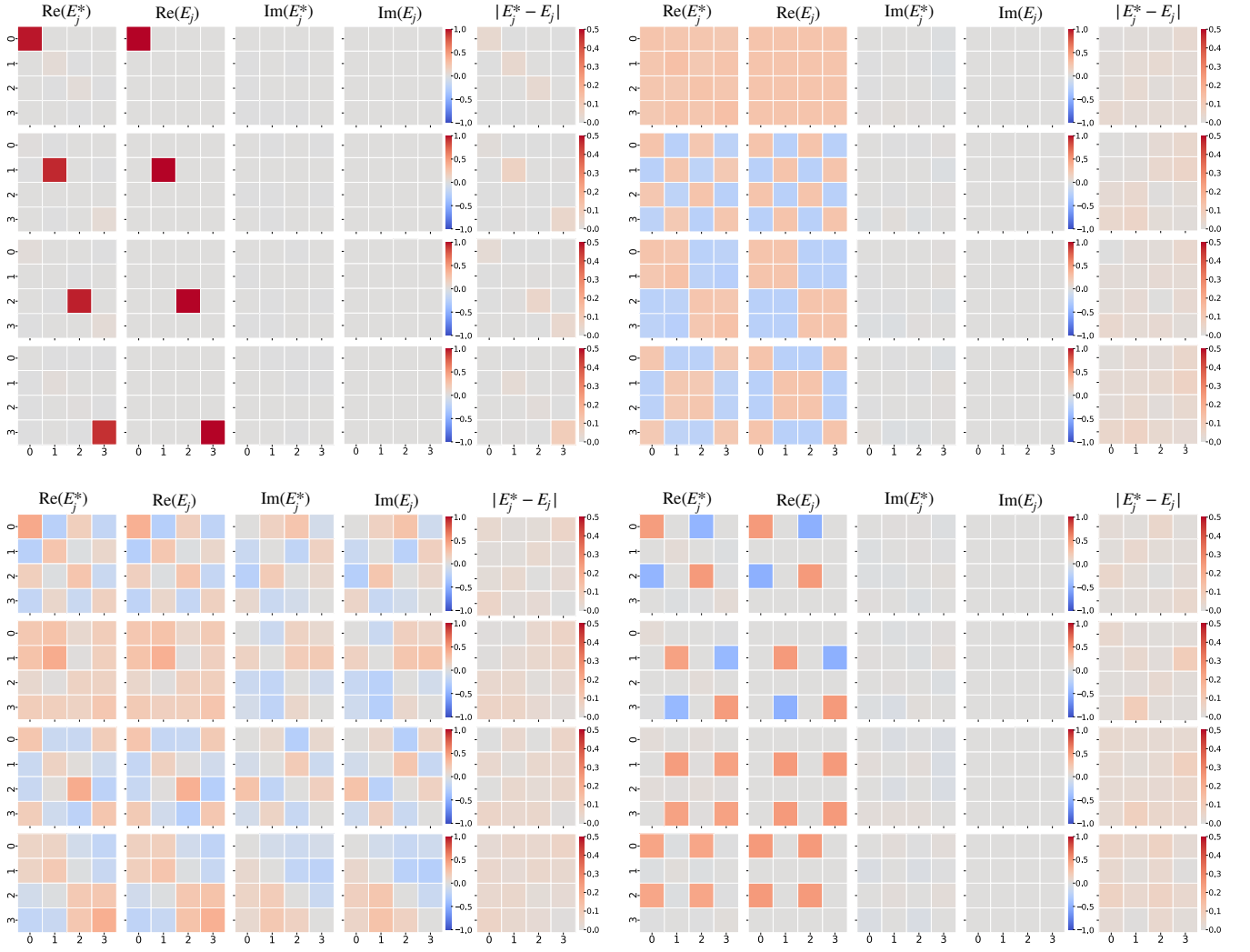


FIG. 6. Results for the reconstruction of various noisy two-qubit POVMs, implemented on a two-qubit flux-tunable transmon device using a budget of  $10^6$  random initial states. The reconstructed noisy POVMs are compared to its expected noiseless counterpart, with the absolute difference displayed. Though noisy, the reconstruction follows the target POVMs closely. The deviations from the expected values are due to the noisy device implementation. More precisely, (top left) depicts the Identity POVM, where only a measurement in the computational basis is performed on both qubits. (top right) depicts a POVM where a Hadamard gate is applied to each qubit before measurement, that is, a change of basis from Z to X measurement basis. (bottom left) POVM where a Haar random gate is implemented before the measurement gate, we notice the how even with a more complex measurement the noisy implementation follows closely the noiseless simulation. Finally, on (bottom right) a Bell type POVM is reconstructed, where unlike the previous three POVMs depicted in this figure, an entangling gate is performed between the two qubits.